Facies and seismic analysis of the Late Carboniferous–Early Permian Finnmark carbonate Platform (southern Norwegian Barents Sea): an assessment of the carbonate factories and depositional geometries.

Authors, affiliation codes and e-mails

Matteo Di Lucia[1]: diluciam@rpsgroup.com

Jhosnella Sayago[2]: sayago@geo.uni-potsdam.de

Gianluca Frijia[2]: gfrijia@geo.uni-potsdam.de

Axum Cotti[3]: axum.cotti@edison.it

Andrea Sitta[3]: andrea.sitta@edison.it

Maria Mutti[2]: mmutti@geo.uni-potsdam.de

1 – RPS Energy, Goldvale House, 27-41 Church Street West, Woking, Surrey, GU21 6DH, United Kingdom.

2 - Institute of Earth and Environmental Sciences, University of Potsdam, Karl-Liebknecht-Strasse 24–25, 14476 Potsdam, Golm, Germany.

3 - Edison Spa, Foro Buonaparte 31, 20121 Milan, Italy.

Acknowledgments

This work was funded through a collaborative research project between the University of Potsdam and Edison International S.p.A., Norway Branch. The Norwegian Petroleum Directorate and Weatherford Norge AS are thanked for providing core access. We thank Sascha Kuske for his help with the data handling in Petrel. We also thank Schlumberger for kindly providing us with PETREL™ licenses and I.

Muench and R. Muschkorgel for providing technical software support. We also thank A. Bohlen (University of Potsdam Transfer GmbH) for his continuous support.

Abstract

The late Palaeozoic buried Finnmark carbonate platform, in the Norwegian Barents Sea, is a depositional system developed under shifting palaeoclimatic and palaeoceanographic conditions. Detailed core analysis from the explorations wells 7128/4-1 and 7128/6-1, combined with 2D seismic sections and data from previous studies in the area have allowed a re-evaluation of the depositional scenarios of the main lithostratigraphic units (Ørn and Isbjørn Formations). Nine lithofacies associations have been described and interpreted in terms of their depositional environments. During the mid-Sakmarian two major changes are observed between the Ørn and Isbjørn Formations: (1) the variation in the type of the carbonate factories and (2) the change in platform morphology. The changes in the types of carbonate factories were controlled by a number of factors and are expressed by changes in biota, facies associations and depositional geometries. The morphological variation has been associated with a change from a distally steepened ramp to a homoclinal ramp. Our results may help to improve the assessment of future evaluations in the Finnmark Platform area, in terms of reservoir properties, which are strictly associated with the depositional styles and their post-depositional modifications.

Introduction

The growth history of a carbonate depositional system, its facies heterogeneity and internal architecture, strictly depend on the interaction of numerous biological, chemical and physical factors, acting at different temporal and spatial scales (Read, 1985; Tucker, 1990; James, 1997; Wright and

47 Burchette, 1996, 1998; Pomar, 2001; Mutti and Hallock, 2003; Schlager, 2003; Bosence, 2005; Pomar
48 and Kendall, 2007). Decades of research on modern and ancient examples have highlighted how
49 sensitive the carbonate platforms are to these changes and how difficult is to interpret their evolution
50 considering all the above-mentioned interplays. This is particularly true for the deeply buried
51 depositional systems, often strongly altered by the diagenetic/structural overprint, which are, only,
52 "imaged" by indirect methods such the seismic. However seismic data may convey artifacts that could
53 results in the inaccurate imaging of platforms real morphologies. A comprehensive understanding of
54 how carbonate platforms develop and change across consecutive phases of their growing history,
55 represents a crucial achievement when economical interests linked to fossil fuels originate, since
56 carbonate rocks host more than half of the global hydrocarbon productive reserves (Schlumberger
57 market analysis, 2007, www.slb.com/carbonates). In the last three decades, numerous studies led to a
58 significant step forward in the understanding of the Arctic regional geology, associated with the
59 increasing offshore exploration in the area (Stemmerik and Worsley, 1989; Cecchi, 1993; Lønøy, 1988;
60 Beauchamp and Desrochers, 1997; Ehrenberg et al., 1998a; Stemmerik and Worsley, 2005; Worsley,
61 2006; Larssen et al., 2005; Colpaert et al., 2007; Rafaelsen et al., 2008). One of the late Palaeozoic
62 geological domains attracting most of the interests of the oil industry is represented by the Finnmark
63 Platform, a buried depositional system of the southern Norwegian Barents Sea (fig. 1a), developed as
64 part of the Arctic epicontinental shelf (Bugge et al., 1995; Stemmerik, 2000; Larssen et al., 2002;
65 Worsley, 2006) and dominated by carbonate deposition (for ~27.5 Ma) during the Late Carboniferous–
66 Early Permian (Gzhelian-Artinskian) (Stemmerik, 1997; Ehrenberg et al., 1998a; Larssen et al., 2002).
67 Among the Late Palaeozoic deposit of this area, the stratigraphic interval corresponding to the Gipsdalen
68 Group is considered as having a high reservoir potential (Ehrenberg, 2004; Stemmerik and Worsley,
69 2005 and references therein) and has been, in recent years, the object of renewed interest for E&P

purposes to assess future possible plays. At the same time, the Finnmark Platform represents a notable example of how the interplay of simultaneous mechanisms of diverse nature, can influence the long-term and large-scale depositional evolution of a carbonate system.

The depositional geometries of the Finnmark carbonates were influenced by the preexistent NE-SW fault-controlled rift topography of the underlying Billefjorden Group (Mississippian clastic sediments), affected by the Devonian-Serpukhovian Atlantic rifting (Stemmerik, 2000; Worsley, 2006). Moreover, during the Late Carboniferous-Early Permian, the Arctic shelf development and its sediment accumulation patterns were influenced by the following major climatic-oceanographic changes:

i) the northward drifting of the Eurasian plate, from tropical (~20°) to temperate (~45°) latitudes, with a rate of about 2-3 mm/y (Scotese and McKerrow, 1990; Scotese and Langford, 1995; Golonka and Ford, 2000) and persistent dry climatic conditions (Stemmerik, 2000).

ii) The presence of the Gondwanan icecaps, whose expansions and retreats phases controlled the cyclicity and magnitude of the sea-level fluctuations (Stemmerik, 2008 and references therein).

iii) The stepwise closure of the Eastern European gateway connecting the arctic regions with the warmer tropical Palaeo-Tethys, influencing successive oceanic circulation patterns (Reid et al., 2007 and references therein).

On the Finnmark Platform, the most remarkable sedimentary expression of such palaeoclimatic and palaeoceanographic changes took place during the middle Sakmarian and records a major shift in carbonate factories (Steel and Worsley, 1984; Stemmerik, 1997; Ehrenberg et al., 1998a; Larssen et al., 2002). Exploration wells and shallow cores within the proximal Finnmark domain, reveal a shift in carbonate production style and accumulation between two major (2^{nd} order) depositional phases of platform development, represented by the photozoan-dominated (*sensu* James, 1997) sequences of the

Gipsdalen Group (Ørn Formation) and the overlying heterozoan carbonates (Stemmerik, 1997; Ehrenberg et al., 1998a; Larssen et al., 2002) of the Bjarmeland Group (Isbjørn Formation).

Although several core- and seismic-based studies have been published so far (Cecchi, 1993; Ehrenberg et al., 1998a; Larssen et al., 2002; Colpaert et al., 2007; Rafaelsen et al., 2008), it is still not fully clear how the Finnmark area evolved in terms of change in geometries and how the early Permian climatic/geodynamic scenario influenced changes in sediment accumulation type. Therefore, for this study, we present the first detailed core analysis across the Asselian-Artinskian Ørn and Isbjørn formations of the wells 7128/6-1 and 7128/4-1 (fig. 4), supported by 2D seismic interpretation across the profile of the eastern Finnmark domain, to better assess the long-term platform evolution and its large scale depositional geometries. This work represent a key study for a more precise reservoir facies evaluation and distribution across the potentially commercial stratigraphic interval of the Ørn Formation (Gipsdalen Group), which is particularly important for the definition of future exploration areas on the Finnmark Platform and on other similar settings of the Barents Sea.

Figure 1 here

Geological evolution and lithostratigraphy

During the Late Palaeozoic, the Arctic shelf lied in the northern margin of the Laurentia super Continent (fig. 1a). It was extended from west to east, from the Arctic Canada across the North Greenland, Svalbard and the Barents Sea, to the Arctic Russia (Beauchamp and Desrochers, 1997, Larssen et al., 2002; Stemmerik and Worsley, 2005; Worsley, 2006). In particular, the late Palaeozoic structural style of the Barents Sea domain derives from Caledonian (NE–SW oriented), and in less extent Timanian

(NW–SE oriented) orogenic lineaments affecting the Pre-Devonian basement (Gabrielsen, 1990; Gudlausson et al., 1998; Samuelsberg et al., 2003). The late Devonian–early Carboniferous separation of the North America from the Fennoscandian craton resulted in a rift-controlled palaeo-topography and development of extensional tectono-stratigraphic provinces dominated by wide shelves (Finnmark and Bjarmeland Platforms), relatively deep basins (Hammerfest, Nordkapp, Bjørnøya, Tromsø Basins), and isolated structural features (Loppa and Stappen Highs) (Larssen et al., 2002) (fig. 1b).

At present, the Late Palaeozoic Finnmark Platform is a buried monocline (gradient of ~2° at the top Permian level, Ehrenberg, 2004) grading northward to the rift-controlled Nordkapp (NE side) and Hammerfest (NW side) Basins (fig. 1b). Southward it is delimited by the Norwegian continent (the Fennoscandian craton) by an angular unconformity. The western boundary is defined by the Ringvassøy-Loppa fault complex whereas eastward the platform gently grades toward the Timan-Pechora Basin (Gudlaugsson et al., 1998; Larssen et al., 2002).

The sedimentary record of the Finnmark Platform starts from the Early Carboniferous. According to Larssen et al. (2002), its Late Palaeozoic stratigraphic evolution has been associated to four distinct depositional phases, corresponding to four lithostratigraphic units: the Billefjorden, Gipsdalen, Bjarmeland and Tempelfjorden Groups (fig. 2). Starting from the Mississippian (early Viséan), the rift-related basement morphologies of the Finnmark area have been gradually filled by continental to marginal marine siliciclastic of the Billefjorden Group (Soldogg, Tettegras and Blaererot formations, fig. 2), deposited under tropical-humid climatic conditions as testified by the common presence of coaly horizons (Larssen et al., 2002). A regional middle Serpukhovian-earliest Bashkirian uplift-related unconformity, associated with reactivation of the underlying structural lineaments of the basement, separates the Billefjorden Group deposits from the overlying early Bashkirian-early Sakmarian Gipsdalen Group. The onset of the Gipsdalen Group deposition is characterized by a shift in the tectonic

138 style, with a progressive reduction of the tectonic activity and increasing subsidence (Gudlaugsson et al.,
139 1998; Larssen et al., 2002; Worsley, 2006). Moreover, in this phase took place a significant
140 palaeoclimatic transition from tropical humid to overall semi-arid to arid conditions, (Stemmerik et al.,
141 2000; Worsley, 2006) testified by a gradual increase of shallow and basinal evaporitic deposits. Finally,
142 the Gipsdalen Group was deposited under high-frequency (100 k.y.) and amplitude (> 50m) glacio-
143 eustatic sea-level fluctuations reflecting the Gondwanan icecaps activity (Stemmerik et al. 2008, and
144 references therein; Koch and Frank, 2011). The Group comprises three formations reflecting distinct
145 sub-phases of the Finnmark Platform evolution. The basal interval is associated with the deposition of
146 continental clastics of the Ugle Formation followed by a widely recognized Bashkirian-Moscovian
147 transgression associated with tectonic subsidence that led to the deposition of the Falk Formation. The
148 latter marks a stepwise shift to mixed continental to shallow marine siliciclastic and carbonates, and
149 deeper subtidal evaporites (fig. 2) (Larssen et al., 2005). Starting from the Gzhelian, the proximal areas
150 of the Finnmark domain were mostly dominated by peritidal to subtidal photozoan
151 limestones/dolostones and minor sabkha evaporites of the Ørn Formation, with periodic occurrence of
152 transgressive heterozoan carbonates. Silty mudstones, gypsum and halite were deposited in the basinal
153 areas (fig. 2) (Larssen et al., 2005; Stemmerik, 2008). The early Sakmarian marks an important regional
154 transition associated with a major melting phase of the Gondwanan ice (Stemmerik, 2008; Koch and
155 Frank, 2011). This led to the termination of the glacio-eustacy and marked the depositional transition
156 between the Gipsdalen Group and the overlying transgressive Bjarmeland Group, entirely dominated by
157 heterozoan carbonates.
158 The Bjarmeland Group is characterized by three laterally transitional formations (fig. 2). The shallowest
159 platform environments show crinoidal-bryozoan carbonates of the Isbjørn Formation whereas the deeper
160 distal shelf areas hosted muddy carbonates and shales of the Ulv Formation (Larssen et al., 2002). Outer

environments were also site of deposition of large buildups complexes of the Polarrev Formation, dominated by bryozoan-*Tubiphytes* and microbial-stromatactis boundstones (Blendinger et al., 1997; Stemmerik, 1997).

From the early Kungurian?-Tatarian?, further northward drifting and cooling, associated with drowning and termination of the temperate carbonate factory on the shelves areas of the Barents Sea, led to the deposition of the outer platform silica- and clastic-dominated Tempelfjorden Group (fig. 2) (Stemmerik, 1997; Beauchamp and Desrochers, 1997; Ehrenberg et al., 1998a; Ehrenberg et al., 2001), composed by the Røye Formation and the Ørret Formation, the latter absent on most of the Finnmark Platform (Larssen et al., 2002).

Figure 2 here

MATERIALS AND METHODS

Stratigraphic Dataset and methods

For this study, we described the late Asselian-late Artinskian stratigraphic intervals cored from the wells 7128/6-1 and 7128/4-1 (fig. 4), both placed in the central-eastern area of the Finnmark Platform domain, at a distance of 26.1 km from each other (fig. 1b). The standard core description has been performed at cm- to dm-scale and followed by the semi-quantitative microfacies analysis on 154 thin sections, mainly focused on the identification of the carbonate/clastic textures, biological content and sedimentary structures. The well depth is given in measured meters (MD) below Kelly Bushing.

The most complete Upper Palaeozoic stratigraphic archive from the subsurface of the Norwegian Barents Sea has been recovered (472.4m of cores/901m of drilled interval) from the exploration well 7128/6-1 (drilled by ConocoPhillips in 1991). It represents the type section for the Ørn Formation (215.3

m-thick) and the overlying Isbjørn (89.4 m-thick) and Røye Formation (117.4 m-thick). The 51.7 m-thick sequence recovered from the exploration well 7128/4-1 (Statoil, 1993) covers the late Asselian-early Sakmarian uppermost interval of the Ørn Formation. A precise stratigraphic correlation between the 7128/4-1 and 7128/6-1 sequences is ensured by the integration of facies analysis, gamma ray log trends and correlative seismic stratigraphic horizons (fig. 3) (Ehrenberg et al., 1998a; Larssen et al., 2002; Colpaert et al., 2007).

Ehrenberg et al. (1998a) defined two 2nd-order and seven 3rd-order depositional sequences (S-1 to S-7) through the Late Carboniferous-Permian interval of the well 7128/6-1 according to the terminology of Goldhammer et al. (1991), bounded by major sequence boundaries (SB) and maximum flooding surfaces (MFS) (fig. 3). Nine lithostratigraphic units (L1-L9) have also been defined by Ehrenberg et al. (2000) on the basis of major vertical facies changes. Units L1-L7 are assigned to the Gipsdalen Gp, whereas the units L8 unit L9 respectively to the Bjarmeland and Tempelfjorden Groups (fig. 3). Fusulinid-based biostratigraphy of the well 7128/6-1 suggests a late Gzhelian to early Sakmarian age for the Ørn Formation, and late Sakmarian to late Artinskian age for the Isbjørn Formation (Ehrenberg et al., 2000 and references therein).

The studied segment from the well 7128/6-1 has a thickness of 104.6m (1850-1745.4m). It covers the topmost part of the Ørn Formation (15.3m) and the entire overlying Isbjørn Formation (89.4m) (figs. 3, 4). The Ørn Formation segment (1850-1834.7m) corresponds to the early Sakmarian uppermost portion of the sequence S-4 of Ehrenberg et al. (1998a) (upper part of the lithostratigraphic unit L-7, fig. 3). The Isbjørn Formation segment (1834.7-1746m) covers the entire late Sakmarian-late Artinskian third-order sequence S-5 of Ehrenberg et al. (1998a) (lithostratigraphic unit L-8). The sequence deepens upward, with the MFS taken at 1813m, and then it shallows up until the boundary with the Tempelfjorden Group (figs. 3, 4).

The studied interval (1865.7-1814m) of the well 7128/4-1 covers most of the third-order depositional sequence S-4 of Ehrenberg et al. (1998a) (lithostratigraphic units L6-L7). The sequence marks a deepening-up trend with a maximum flooding surface (MFS) at 1837.7m, followed by shallowing up to the end of the cored interval (figs. 3, 4). For a better understanding of the depositional-sedimentological features of the Finnmark areas, we also used other available Palaeozoic stratigraphic data, including cores from the exploration wells 7228/9-1S (drilled by Norsk Hydro in 1989) and 7229/11-1 (drilled by Shell in 1993), located in a more distal position, and the shallow bore holes 7128/12-U-01, 7129/10-U-01 and 7030/03-U-01 (IKU Petroleum Research, 1987-1988) drilled landward the studied wells, closer to the Norwegian coast (fig. 1b).

Figure 3 here

Seismic Dataset and Seismic Stratigraphy

The 2D seismic line 213 from the survey ST9715 has been used for seismic interpretation (fig. 10a). The line is 97 km-long and oriented in NE-SW direction, covering a proximal-distal transect of the eastern Finnmark Platform (see figs. 1 and 10 for location). The frequency values of the 2D line range from 20 to 50 Hz, with a dominant frequency of 25 Hz. The internal velocities of the carbonate interval range from 4000 to 6000 m/s, therefore the vertical seismic resolution fluctuates between 40 to 60 m (according to the dominant frequency). Seismic vertical scales are given in two-way travel time TWT (in seconds). The seismic-well tie was done by creating synthetic seismograms that allowed identification of main reflectors in the wells 7128/4-1 and 7128/6-1, as summarized in figure 3. Reflector continuity and key stratal terminations have been considered to identify and mark the selected seismic reflectors and to develop a sequence stratigraphic model along the 2D line (fig. 10b-c). Different seismic attributes (i.e. frequency band filter, variance, gradient magnitude) were applied to highlight the stratal terminations

and eventual major structural discontinuities. To facilitate comparisons with previous works based on the same dataset, we followed for the interpreted seismic horizons the nomenclature adopted by Colpaert et al. (2007). The Middle Carboniferous Horizon (MCH) marks the boundary between the Billefjorden and the Gipsdalen Groups and reflects the middle Serpukhovian-earliest Bashkirian major uplift and erosional event. The reflector can be well recognized across the platform since it shows evident truncation of the underlying eroded clastic reflectors (fig. 10b-c). MCH delimitates the base of the seismic unit SU1 of Colpaert et al. (2007) (fig. 3). Upwards, the Middle Gzhelian Horizon (MGH) has been traced. It correlates with the top of the depositional sequences S-2 of Ehrenberg et al. (1998a), thus matches the third-order sequence boundary following the Gzhelian highstand and the onset of the Ørn Formation. MGH marks the top of the seismic unit SU1 of Colpaert et al. (2007) (fig. 3). Following upwards, the Upper Asselian Horizon (UAH) has been selected. It correlates with the second-order sequence boundary at the top of the depositional sequence S-3 (fig. 3) and represents the top reflector of the seismic units SU3 of Colpaert et al. (2007). Upwards, the Middle Sakmarian Horizon (MSH) has been marked and corresponds to the boundary between the Ørn and the Isbjørn Formation (Gipsdalen Group-Bjarmeland Group) (fig. 3). It correlates with the third-order sequence boundary at the top of the depositional sequence S-4 and marks the top of the seismic unit SU4. Evident onlap terminations above MSH in the marginal areas reflect the early transgressive character of the Isbjørn Formation on the platform (fig. 10b-c). The last selected reflector corresponds to the Base Kungurian Horizon (BKH) marking the top of the Bjarmeland Group. It correlates with the third-order sequence S-5 of Ehrenberg et al. (1998a) and marks the top of the seismic unit SU5 (fig. 3).

RESULTS AND INTERPRETATION

Core Description and Facies Analysis

The studied cores are dominated by carbonates (limestones and subordinate dolostones), with minor occurrence of calcareous sandstones, calcareous shales and evaporites (fig. 4). Core description and microfacies analysis allowed defining nine lithofacies associations (LA1–LA9), mainly based on lithology, textures, skeletal/non-skeletal components and sedimentary structures. The facies nomenclature follows at large the first description of the two wells given by Ehrenberg et al. (1998a), as well as other facies studies performed in adjacent coeval deposits of the Arctic region, as in the Svalbard and Sverdrup areas (Beauchamp and Desrochers, 1997; Hüneke et al., 2001; Reid et al., 2007; Blomeier et al., 2009, 2011). Major erosive surfaces are always associated through the cores with distinct mm- to cm-thick silty-clayey partings. Here, due to lack of diagnostic sedimentary/diagenetic features, it is often complicated to assess if such surfaces are associated to phases of subaerial exposure and/or submarine erosion/non sedimentation. However, the vertical facies changes allowed detecting meter-scale (up to 8m) subtidal to peritidal shallowing-up (SU) and deepening-up (DU) cycles, defined across the Ørn Formation segment of both the wells, as shown in figure 4. Contrarily, across the Isbjørn Formation of the well 7128/6-1 is difficult to identify a precise stacking pattern and record of depositional cyclicity higher than the 3rd order of Ehrenberg et al. (1998). One reason could be that the Isbjørn Formation was mainly deposited within subtidal settings and under low frequency/amplitude sea level fluctuations. Moreover, the original record of depositional cycles given by facies variations (LA8-LA9) has been further obliterated by burial compaction.

Figure 4 here, full page

Lithofacies Associations (LA)

LA1 - Nodular Anhydrite

This lithofacies is characterized by a mosaic of mm-/cm-sized sub-rounded and elongated nodules of anhydrite, referable to the typical "chicken-wire" and "entherolitic" fabrics (Butler, 1970; Ciarapica et al, 1985; Warren, 2006, and references therein), in a mixed dolomitic and fine sandy to silty matrix (fig. 5a). In place the nodules are densely packed and surrounded by thin stylonodular seams as probable result of burial compaction. The lack of thin sections did not allow more detailed petrographic characterization. However, from hand lens observation no faunal content has been detected in the matrix. LA1 occurs as a 1.4 m-thick bed in the studied interval of the well 7128/4-1 (fig. 4) and is interpreted as associated to sabkha-dominated supratidal depositional settings.

LA2 – Dolomitic Mudstones

The microfacies is characterized by partially to highly dolomitized mudstones to pure fine crystalline dolostone. Scattered mm- to cm-sized anhydrite nodules are visible (fig. 6a) and arranged parallel to the bedding. They show occasionally an "entherolitic-like" fabric and are at times associated with dolomitized mm-thick laminae. Some dm-thick horizons are completely barren and in place alternated with interval characterized by horizontal fenestral-like structures. Sparse fine-grained sub-rounded quartz grains and isolated peloids of possible microbial origin are common, together with cm-sized chert nodules of diagenetic origin. Faunal content is rare and is made of thin-shelled ostracods and small encrusting foraminifera. This lithofacies caps at times the SU cycles of the 7128/4-1 core (at 1858.9, 1853.7 and 1840.5m, fig. 4) and it occurs frequently across the middle Gzhelian and middle Asselian intervals of the well 7128/6-1, associated to the third-order SBs of the sequences S-2 and S-3 of Ehrenberg et al. (1998a) (fig. 3). LA2 is interpreted as deposited in a restricted intertidal hypersaline environment, associated with marginal marine tidal flat/lagoonal settings.

LA3 – Fine-grained calcareous Sandstones

This microfacies (fig. 6b) consists of fine-grained, sub-angular to sub-rounded, moderately- to poor-packed and well-sorted quartzose sandstone, including a lesser amount (up to 30 %) of bioclastic fragments of diverse nature, at times completely recrystallized. The intergranular pore spaces are partially occluded by blocky calcite and minor anhydrite cement. The bioclastic content shows fragments of rugose corals, bryozoans and green algae; rare small foraminifera, calcispheres and ostracods are also observed. Non-skeletal grains are represented by rare microbial peloids and muddy lithoclasts. LA3 has a limited occurrence within the studied Ørn Formation interval of both the wells. Two 1.5 and 1.1 m-thick beds have been recognized in the lower and upper part of the 7128/6-1 core (respectively at 1945.5 and 1937.2m, fig. 4). A 0.7 m-thick bed occurs at the top of the core 7128/4-1 (1814.7m, fig. 4) (the top of this bed is undefined due to lack of cores upwards). The bedding shows poor-marked parallel to low angle planar cross-laminae, massive horizons and pseudo-bedding due to stylonodular seams of burial origin. LA3 is vertically alternated with bioclastic grainstones (LA5) and has been interpreted as deposited in a sand flat/beach environment, ranging intertidal to shallow subtidal settings, above the FWWB. According to Ehrenberg et al., (1998a), these fine-grained clastics record transport from the land during shoreline progradational phases. Successive washing and sorting by the waves and currents action helped the mixing with shoal/lagoonal-derived skeletals and the removal of the muddy component.

LA4 – Bioclastic Wackestone-Packstones

The microfacies shows massive beds of wackestone to packstone textures with moderate to high faunal diversity in a micritic/microsparitic matrix, in place partially to highly dolomitized or with a clotted fabric. The most common taxa are represented by small foraminifera and calcareous algae (fig. 6c-d).

The foraminifera refer to globular encrusting and benthic forms as tuberitinids, globivalvulinids, apterinellids, as well as *Tetrataxis* sp., textulariids and bradyinids. Larger fusulinids are less frequent. The calcareous algae are mainly represented by epistamoporids (*Epimastopora* sp.) and minor beresellids. Common subordinate bioclastic variety includes fragments of rugose corals, *Palaeoaplysina*, incrustations of the microproblematica *Tubiphytes* sp., *Girvanella* sp. and *Ellesmerella* sp., red algae (*Komia* sp.), bryozoans, crinoids, ostracods and rare calcispheres. Non-skeletal grains are represented by peloids and rare oncoids. Fine-grained quartz grains are common. This lithofacies occurs frequently in the Ørn Formation interval of both the cores (fig. 4).

LA4 is interpreted as deposited in subtidal (below the FWWB) and partially protected lagoonal settings as shown by the presence of mud and the associated high faunal diversity. Such environment was strictly interconnected with sand shoals (LA5) and skeletal buildups (LA6).

LA5 – Bioclastic Grainstones

The microfacies is made of fine to coarse grainstones that appear in core poorly to highly cemented, either massive or showing slightly inclined bedding within few horizons. The microfacies is characterized by moderate to highly diversified biota, often fragmented and recrystallized. It is comparable with LA4 as relative abundance among the different taxa. It is mainly composed of smaller foraminifera (encrusting and small benthic forms), fragments of green algae (*Epimastopora* sp.), *Palaeoaplysina*, rugose corals and bryozoans, encrustations of *Tubiphytes* sp., *Girvanella* sp. and *Ellesmerella* sp. Subordinate are red algae (*Komia* sp.), calcispheres, monoaxon sponge spicules and crinoidal fragments. Non-skeletal grains are represented by peloids and rare oncoids (fig. 6e-f). LA5 occurs frequently across the Ørn Formation of both the studied cores (fig. 4).

LA5 is interpreted as a shoal-dominated shallow subtidal environment, placed around the FWWB and dominated by high hydrodynamic regime that contributed to wash away the muddy sediments through a constant wave action. The clear similarity in the overall skeletal content, plus the frequent vertical transition between LA5, LA4 and the buildup facies of LA6, suggests a strong depositional interaction between these facies. Therefore, we assume that the LA5 represent the reworking of both the muddy lagoonal textures (LA4) and the biostrome debris (see LA6).

LA6 – Skeletal Boundstones

It is considered as a composite lithofacies association comprising dm- to m-thick boundstones, dominated by different categories of reef-builders. They are mainly made by *Palaeoaplysina* grains (LA6a) and rugose colonial corals (LA6b), associated with minor phylloid algae (fig. 4). Rare are bryozoans and tabulate corals colonies. LA6 occurs within both the sections and is named following Ehrenberg et al. (1998a).

LA6a – Palaeoaplysina Boundstones

The facies is made of mm-thick slightly undulated plates of *Palaeoaplysina*, mostly horizontal and occasionally inclined up to 30°, forming a skeletal framework that baffles/traps sediments. The interstitial space (fig. 6b) is generally made of subtidal wackestone-packstones (LA4), at times dolomitized and occasionally alternated with bioclastic grainstones (LA5), suggesting variations of the hydrodynamic regime associated with the buildup growth. In some cases, the internal structures of *Palaeoaplysina* are often almost completely reset by diagenetic overprint related to meteoric leaching, insomuch that it is difficult to discriminate primary textures. *Palaeoaplysina*-boundstones (figs. 5b, 7a) reach a thickness of about 2m in the 7128/4-1 core. They do not occur within the studied segment of the

367 well 7128/6-1 but are recurrent (and up to 6.7 m-thick) through the underlying Gzhelian-Asselian
368 interval, making most of the lithostratigraphic unit L-4 of Ehrenberg et al. (1998a, fig. 3).
369 *Palaeoaplysina* was a major reef-builder of the Late Carboniferous-Early Permian (Wahlman, 2002;
370 Nakazawa et al., 2011). Its taxonomic affinity is still under debate and so far has been ascribed to
371 sponges (Krotov, 1888; Flügel, 2004), stromatoporoids (Stuckenberg, 1895), hydrozoans (Davies, 1971)
372 and green algae. The latest affinity (Vachard and Kabanov, 2007) considers *Palaeoaplysina* as
373 Archaeolithophyllacean red algae.
374 Outcrop analogs of Late Carboniferous-Early Permian *Palaeoaplysina*-dominated buildups have been
375 widely described across the entire northern Pangaea margin (Skaug et al., 1982; Breuninger et al., 1989;
376 Beauchamp and Desrochers, 1997; Stemmerik et al., 1994, 1999; Morin et al., 1994; Bugge et al., 1995;
377 Hüneke et al., 2001; Wahlman, 2002; Stemmerik, 2003; Reid et al., 2007; Blomeier et al., 2011). These
378 works describe such bio-constructions as having different size, morphology and subordinate faunal
379 associations, depending on the interactions between depositional and tectono-stratigraphic settings in
380 which they were growing (Wahlman, 2002; Stemmerik, 2003). This could suggest that the growth of
381 *Palaeoaplysina* was not tied to specific environmental conditions. However, the composition of the
382 subordinate faunal associations (mostly light-dependent organisms) always limits the development to the
383 shallow photic zone. In fact, it has been generally assumed that the growth of m-thick (up to 10m)
384 isolated patches and lenticular laterally-developed banks (up to 100s m-wide) was favored by the
385 reduced accommodation within inner platform environments. In turn, stacked and thicker complexes
386 could have been formed in deeper subtidal settings but always within the photic zone (see Wahlman,
387 2002 for a review). It has been also suggested that, although *Palaeoaplysina* communities did not
388 "despise" agitated conditions (see also Breuninger et al., 1989 and Davies, 1989), they likely preferred
389 to colonize the substrate of more open subtidal settings of the inner/middle ramp areas (Hüneke et al.

2001). *Palaeoaplysina* boundstones are interpreted here as forming isolated banks, growing within inner to middle ramp settings. The dominance of interstitial muddy textures (L4-like) suggests buildups development below the FWWB under moderate hydrodynamic settings, with periodic enhanced water dynamism testified by the interstitial grainstones.

Occasionally, platy and cup-shaped recrystallized *Eugonophyllum* phylloid algal fragments (Udoteacean and Halimedacean algal affinity; see Forsythe et al., 2002 and reference therein) occupy interstitial cavities among the *Palaeoaplysina* plates, suggesting the presence of colonies in nearby areas. Phylloid algae are not common within the studied intervals but are frequently associated with *Palaeoaplysina* in the lower part of the unit L-4 of the well 7128/6-1, dominated by buildups (fig. 3). *Eugonophyllum* phylloid algae represent widespread tropical-subtropical reef-builder organisms across the Moscovian-Sakmarian time (Wahlman, 2002). In general, the size, morphology and associated fauna of such bio-constructions do not differ from the *Palaeoaplysina*-dominated ones. Therefore, their development has been frequently described within analogous or transitional environmental settings (Bugge et al., 1995; Ehrenberg et al., 1998a; Morin et al., 1994; Stemmerik et al., 1999; Hüneke et al., 2001; Wahlman, 2002; Stemmerik, 2003; Nagazawa et al., 2011). Among the two, the more fragile structure (faster growing mode) of the *Eugonophyllum* colonies could have made them preferring quieter (more protected or deeper) environments to colonize the sea bottom (Morin et al., 1994 and references therein).

LA6b – Coral/Bryozoan Boundstones

Coral boundstones are present in the Ørn Formation interval of both the studied sections. Differently from the *Palaeoaplysina*-phylloid algal boundstones, their occurrence across the Gzhelian-Asselian L-4 Unit of the well 7128/6-1 is limited (Ehrenberg et al., 1998a; Larssen et al., 2002). In the studied intervals, they are arranged in massive cerioid (fig. 5c) or phaceloid (fasciculate structure of separated

circular corallites, fig. 5d) colonies of rugose and rare tabulate (syringoporid) corals, reaching up to 1.6m. The inter-corallite spaces (fig. 6h) are mostly occupied by coarse-grained packstones-grainstones of LA4 and LA5, with a very variable fauna but prevalence of broken bio-eroded coral fragments, smaller encrusting foraminifera, *Tubiphytes* sp., *Girvanella* sp., *Ellesmerella* sp., bryozoan fragments and micropeloids. Sometimes, intra-corallite dissolution vugs are filled by chert and anhydrite cements. In the studied intervals, the rugose coral colonies are commonly overlain by subtidal muddy facies (LA4 and LA7) and occupy the top of the SU cycles. In fact, compared with the *Palaeoaplysina* boundstones, these small patches seemed to have been subjected to greater or at least more constant hydrodynamic regimes which could have been responsible for a more efficient mud removal from interstitial cavities. Therefore, the coral boundstones are interpreted as forming small scattered isolated patches of colonies thriving in a shallow subtidal inner ramp environment.

LA7 – Fusulinid Wackestone-Packstones

This lithofacies is made of wackestone-packstones and sporadically packstone-grainstones with moderate faunal diversity and prevalence of fusulinids foraminifera (fig. 7c-d). The bedding style range from massive to nodular (with increase of the fusulinid shelliness usually associated to horizons showing greater burial compaction) and some horizons show a preferred orientation of the biotic components, possibly related to transport by subtidal current. Subordinate skeletal content is often fragmented and shows common small benthic foraminifera (mainly *Tetrataxis* sp.), bryozoans and crinoids. Minor component are represented by *Palaeoaplysina grains*, rugose corals, *Tubiphytes* sp. and brachiopods. ?*Eugonophyllum* fragments, trilobites and monoaxon sponge spicules are rarely observed (plate 2c-d). The matrix is occasionally dolomitized and appears as micritic to microsparitic to pseudosparitic, including common silty-grained quartz and glauconite. Lithofacies LA7 occurs sporadically at the base

436 of the SU cycles within both the studied cores (fig. 4). LA7 is interpreted as deposited in a subtidal open
437 middle ramp environment, below the FWWB.
438
439 **LA8 – Crinoidal-Bryozoan Grainstones**
440 The lithofacies shows massive beds of fine to coarse-grained bioclastic grainstones and sporadically
441 rudstones with a low to moderate faunal diversity, dominated by fragments of bryozoans (mostly
442 cystoporid) and crinoids (fig. 7e-f). Secondary skeletal content comprises variable proportions of
443 brachiopods, fusulinids, siliceous sponges (entire and disarticulated in monoaxon spicules) and
444 *Tubiphytes* sp.. Rare small foraminifera, ostracods and trilobites fragments are found, as well as sparse
445 glauconitic mm-sized grains. High-amplitude stylolites and other pressure-solution features are
446 frequently observed on core, together with sporadic cm- to dm-sized roundish chert nodules. This LA
447 occurs in the upper part of the 7128/4-1 Ørn Formation (the interval between 1834m and 1821m) and
448 dominates, together with LA9, the overlying Isbjørn Formation of the 7128/6-1 core (fig. 4). The LA8
449 grainstones were likely deposited in subtidal open marine settings, above and/or around the SWB (distal
450 middle ramp). The dominant fabric of reworked and disarticulated skeletals, point out toward areas
451 characterized by open circulation, affected by currents and storms that possibly contributed to
452 accumulate mud-free bioclastic debris.
453
454 **LA9 – Crinoidal-Bryozoan silty Wackestone-Packstones**
455 This lithofacies is characterized by nodular bioclastic wackestone-packstones and rarely floatstones,
456 bioturbated, dominated by disarticulated crinoids and bryozoans (figs. 5f, 7g-h). The matrix is micritic to
457 calcisiltitic and becomes silty/clayey-rich within the most nodular intervals, showing irregular
458 proportions of very fine sub-rounded quartz grains and less micas, plus mm- to cm-sized glauconitic

grains. Subordinate faunal content is represented by variable proportions of brachiopods, monoaxon sponge spicules, mollusk fragments and rare *Tubiphytes* sp. and fusulinid foraminifera. The nodular aspect of LA9 is given by the ubiquitous presence of compaction and burial dissolution. This process favored the accumulation of silty-clayey-dominated horizons following carbonate dissolution (Ehrenberg, 2004). This lithofacies association is gradually to sharply alternated with LA8 in the upper part of the 7128/4-1 core and across the entire Isbjørn Formation of the 7128/6-1 core (fig. 4). LA9 represents the transition towards the basin of the LA8 grainstones and is interpreted as deposited within subtidal open marine outer ramp settings (below the SWB). The chaotic fabric of some horizons might reflect reworking and accumulation under storm conditions within the proximal outer ramp areas, whereas in the more distal outer ramp, the size and amount of the bioclastic fragments decreases and wackestones prevail on packstones.

Figures 5, 6 and 7 here. Figures 6, 7 full page.

Well 7128/4-1 Section

The studied interval of the 7128/4-1 well section is organised in eleven m-scale subtidal to peritidal cycles. The lower 12.7m (1865.7-1853m) of the section comprise the first 4 depositional cycles and show regular alternation of bioclastic grainstones (LA5), bioclastic wackestones-packstones (LA4) and foraminiferal wackestones (LA6), capped at the cycle tops by dolomitic mudstones (LA2). Upwards (until 1843m) the next two cycles comprise bioclastic grainstones (LA5) and bioclastic wackestones-packstones (LA4) overlain at the cycle tops by skeletal boundstones (LA6). From 1843m to 1839.1m bioclastic wackestones-packstones (LA4) are overlain by nodular anhydrite (LA1) whereas in the next cycle (up to 1833m) bioclastic grainstones (LA5) are alternated with foraminiferal wackestones (LA7)

and skeletal boundstones (LA6), followed by the deepening-up segment represented by crinoidal-bryozoan nodular packstone-wackestones (LA9). In the next cycle the LA comprise crinoidal-bryozoan grainstones (LA8), bioclastic wackestones-packstones and grainstones (LA4-LA5) and *Palaeoaplysina*-phylloid algae boundstones (LA6). These LAs are followed by nodular dark calcareous clay-siltstones that represent the deepening-up segment and mark the 3rd order MFS of the sequence S-4 of Ehrenberg et al. (1998a) (figs. 3, 4). Upward the LA shallow-up again; crinoidal-bryozoan silty wackestone-packstones (LA9) are followed by crinoidal-bryozoan grainstones (LA8) and bioclastic grainstones (LA5). The last cycle (1820.4-1814m) is again dominated by bioclastic wackestones-packstones (LA4), shoaling-up to bioclastic grainstones (LA5) and alternated with two skeletal boundstones *Palaeoaplysina*-dominated beds (LA6). At its top the last cycle shows 70cm of calcareous sandstones (LA3).

Well 7128/6-1 Section

The studied interval of the 7128/6-1 well section assigned to the Ørn Formation is organised in 5, m-scale, subtidal to peritidal cycles. The first cycle shows bioclastic packstones (LA4) followed by about 1.5m of calcareous sandstones (LA3) that can be correlated with the sandstones bed at the top of the 7128/4-1 section (Ehrenberg et al., 1998a, fig. 4). Above the cycle deeps-up, as the sandstones are overlain by bioclastic packstones (LA4) and fusulinid wackestone-packstones. The following two cycles (from 1847.5m to 1839.3m) are dominated by foraminiferal wackestones-packstones (LA7) and bioclastic grainstones (LA5), overlain at the cycles top by skeletal boundstones (LA6). The last two SU cycles are represented by bioclastic grainstones (LA4); calcareous sandstones (LA3) cap the top of the first cycle.

The shift to the Isbjørn Formation (at 1834.7m) is associated with an erosional surface at the top of the bioclastic grainstones (fig. 5e), followed by about 5 cm of nodular silt that pass upward to massive crinoidal-bryozoan grainstones (LA8). This level corresponds to the 3rd order SB of the sequence S-4 of Ehrenberg et al. (1998a) (fig. 3). The interval (1834.7m to 1746m of the well 7128/6-1) is dominated by an alternation of crinoidal-bryozoan grainstones (LA8) and subordinate nodular crinoidal-bryozoan wackestone-packstones (LA9). The first 4.5m show massive grainstones (LA8). Upwards, the nodular LA9 prevails on LA8, showing an overall deepening trend up to 1813m. Here, a 70 cm-thick calcareous shaly wackestone bed marks the MFS of the sequence S-5 of Ehrenberg et al. (1998a) (fig. 4). Upwards, the section is dominated until the top by grainstones (LA8) with sporadic occurrence of nodular wackestone-packstones (LA9). In the topmost 20cm of the section, nodular packstones show centimetric bioturbation cavities filled by micro-breccia, in a matrix of greenish silt. The last 10cm are completely brecciated and capped above an erosional contact by the overlying calcareous shales of the Tempelfjorden Group.

The presence of an early-middle Sakmarian stratigraphic hiatus marking the boundary between the Gipsdalen and Bjarmeland Groups is observed at regional scale, affecting with a slight different temporal occurrence structural highs and most of the proximal depositional areas of the Arctic domain (Stemmerik and Worsley, 2005 and references therein). However, the duration of such gap seems to reflect local settings. It is associated with karst features in Spitsbergen, Bjørnøya and North Greenland (Stemmerik et al., 1996, 1997; Worsley et al., 2001; Stemmerik and Worsley, 2005), whereas the corresponding erosional surfaces from the wells 7128/6-1 and 7129/10-U-02 (IKU shallow core) of the Finnmark Platform (fig. 1 b) are devoid of evidences of subaerial exposure (Bugge et al., 1995; Ehrenberg et al., 1998a) and may correspond to a relatively short period of non deposition and submarine erosion prior to the following major transgression. As stated also by Groves and Wahlman

(1997), the carbonate succession from the core 7128/6-1 was characterized by cyclic hiatuses, which are below the resolution of the fusulinid-based biostratigraphy.

DISCUSSION

Carbonate factories and depositional palaeoenvironments

Following previous classifications (Lees and Buller, 1972; Nelson, 1988a, b), Beauchamp (1994) introduced a specific nomenclature for the Palaeozoic biotic/abiotic associations that consider temperature-controlled sediment distributions based on palaeolatitudal and palaeobathymetric variations (see also Beauchamp and Desrochers, 1997). Such nomenclature includes the following sedimentation modes: Chloroforam (dominated by calcareous algae and benthic foraminifera), Bryonoderm-extended (dominated bryozoan and echinoderms, plus subordinate Chloroforam components) and Bryonoderm (dominated by bryozoans, echinoderms, brachiopods and siliceous sponge spicules). In view of the close affinity with the faunal associations found in this study, the Chloroforam, Bryonoderm-extended and Bryonoderm modes will be used instead of the general warm-, mixed and cool-water sedimentation modes respectively.

According to our microfacies analysis, the Asselian-early Sakmarian marine interval of the Ørn Formation records inner to outer ramp deposits (fig. 8a). Diversified associations dominated by small benthic foraminifera, green algae and encrusting communities, thrived in the shallowest, photic, warm inner ramp areas, characterized by intertidal sabkha/tidal flats, subtidal partially protected lagoons, shallow sandbars and m-thick buildup patches dominated by *Palaeoaplysina* and rugose corals. From the middle ramp downward, light-dependent communities are stepwise replaced by a mixed, Bryonoderm-extended fauna. Here, fusulinids and minor *Palaeoaplysina*, rugose and tabulate corals, were associated with typical heterozoan taxa as bryozoans and crinoids (LA7). Finally, the outer ramp

550 domains were dominated by the growth of heterozoan Bryonoderm communities (bryozoans, crinoids,
551 brachiopods).

552 Comparable lateral facies trends have been also observed in the Ørn Formation of the proximal
553 shallow cores 7030/03-U-01 and 7129/10-U-02 (Bugge et al., 1995 and Ehrenberg et al., 2000). In
554 addition, similar variations of the facies patterns with water depth (from photozoan to heterozoan) have
555 been suggested for many other coeval Arctic neritic domains of the Arctic shelf (Kleilen, 1992; Morin et
556 al. 1994; Beauchamp and Desrochers, 1997; Hüneke et al., 2001; Reid et al., 2007; Blomeier et al.,
557 2011).

558 The sedimentary record of the most distal and deepest environments of the Finnmark domain
559 during the deposition of the Ørn Formation is given by cores from the wells 7228/9-1S and 7229/11-1
560 (fig. 1, black circles). They are characterized by transgressive silty nodular mudstones alternated with
561 lowstand subtidal evaporitic sequences. The evaporites are associated with intervals of increased
562 restricted conditions and isolation of the Nordkapp Basin (Larssen et al., 2002; Rafaelsen et al., 2008;
563 Stemmerik, 2008) and possibly correlate, in the well 7128/6-1, with the lithostratigraphic units L-3 and
564 L-5 (dominated by dolomitic mudstones and marked by the major sequence boundaries S-2 and S-3 (fig.
565 3; Ehrenberg et al., 1998a; Colpaert et al., 2007).

566 Starting from the middle Sakmarian, the deposition of the Bjarmeland Group marks a significant
567 change in the sediment accumulation type. The studied cores (fig. 4) from the Isbjørn Formation reveal
568 that the Finnmark became site of deposition of pure heterozoan facies also in the proximal areas,
569 reflecting a landward transition of the Bryonoderm sedimentation mode. According to our facies
570 analysis and previous interpretations of the core 7128/6-1 (Ehrenberg et al., 1998a), the schematic facies
571 model of figure 8b shows a general ramp profile where inner-middle ramp storm influenced areas were
572 occupied by crinoidal-bryozoans grainstones (LA8) and, below the SWB, by the mud-dominated

573 nodular textures of the LA9. The coeval interval (sequence S-5) from the shallow cores 7129/10-U-02
574 and 7128/12-U-01 is thinner (bout 45m vs. 89.4m in the well 7128/6-1) and dominated by the skeletal
575 grainstones (similar to our LA8), suggesting shallower conditions, less accommodation and presence of
576 stratigraphic hiatuses due to lack of biozones (fusulinid zone 20) (Bugge et al., 1995; Ehrenberg et al.,
577 2000). Seaward, cores from the well 7229/11-1 show that the outer ramp domains were at the same time
578 site of deposition of hundreds of m-thick stacked buildups made up by bryozoans and *Tubiphytes*
579 assemblages of the Polarrev Formation (not shown in figure 8b; Blendinger et al., 1997; Stemmerik,
580 1997; Larssen et al., 2002), forming an evident and mostly continuous ridge easily detectable on seismic
581 (fig. 9). Deeper silty mudstones of the Ulv Formation were deposited around the buildup belt and
582 basinward.
583
584 Figure 8 here
585 ---
586
587 **Factors affecting the shift in carbonate factories**
588 Photozoan vs. heterozoan modern sediments distribution essentially varies with respect to sea-water
589 temperature and depth, latitude and circulation patterns (Lees and Buller 1972; James 1997; Mutti and
590 Hallock, 2003) that in turn, also regulate the trophic resources distribution by upwelling across the shelf.
591 The evolution of the Finnmark Platform as part of the huge shallow Arctic epicontinental shelf was
592 affected by northward drifting of the Eurasian plate with a rate of 2-3 mm/year (Scotese and McKerrow,
593 1990; Scotese and Langford, 1995; Golonka and Ford, 2000). During the deposition of the Ørn
594 Formation (Gzhelian–Sakmarian) the Barents Sea domain was still placed within the (sub-) tropical belt
595 (20°–30°) and was associated with high frequency (100 k.y.) and amplitude (>50m) glacio-eustatic sea-

596 level variations (Stemmerik, 2008). Moreover, the palaeogeographic scenario suggests open current
597 circulation patterns due to the NW-SE connections between the Panthalassa and the Palaeo-Tethys
598 Oceans, through the Uralian seaway (fig. 1a) (Reid et al., 2007; Blomeier et al., 2009).
599 On the base of these assumptions and considering the sedimentary records of the Sverdrup Basin, the
600 Svalbard archipelago and Easter European Platform, has assumed that the Late Carboniferous-earliest
601 Permian sedimentation patterns across the Arctic domain were influenced by prevalent circulation of
602 wind-driven oligotrophic warm waters at the surface, from both the Tethys and Panthalassa Oceans
603 (Reid et al. 2007). Therefore, the presence of a stable thermocline during the Moscovian-Sakmarian is
604 suggested to explain the widespread development of shallow photozoan biota (associated with
605 supra/intertidal evaporites in the most restricted areas), separated by deeper heterozoan mesotrophic
606 associations within the same depositional systems. Such hypothesis is consistent with our
607 palaeoenvironmental interpretations (fig. 8a) that consider (sub-) tropical latitude and a depth-related
608 transition in carbonate factories across the Ørn Formation sedimentary record of the Finnmark Platform.
609 From the late Sakmarian, the onset of a Bryonoderm sedimentation mode was established on the
610 Finnmark Platform and across the Arctic province (Stemmerik, 1997). Such significant modification in
611 the depositional style is commonly associated to the effect of: i) an early Sakmarian flooding event
612 during a major melting phase of the Gondwanan icecaps (Stemmerik, 1997; Stemmerik et al., 2008 and
613 references therein); ii) the generalized cooling due to further northward drifting of the Arctic shelf up to
614 the temperate latitudinal belt (Stemmerik, 1997); iii) the stepwise closure of the Uralian corridor
615 connecting the tropical Tethyan waters with the Arctic seas (Fokin et al., 2001; Reid et al., 2007 and
616 references therein).
617 The interplay of such mechanisms led to a new climatic-oceanographic Arctic scenario, characterized by
618 temperate and more seasonal climatic conditions associated with a low frequency/amplitude of the sea-

level cyclicity and a generalized subtidal open marine storm-affected sedimentation. Such circumstances possibly contributed to weaken the water masses stratification, resulting in a disruption of the thermocline and consequent upwelling and influx of panthalassic nutrient-rich cool waters across the entire Arctic shelf (Beauchamp and Baud, 2002; Reid et al., 2007). The result was the ultimate turnover in favor of heterozoan assemblages that from the late Sakmarian invaded also the more proximal and shallow environments, and dominated them up to the Kungurian time.

Besides cooling and upwelling-driven mesotrophic conditions, enhanced nutrients delivery through siliciclastic continental run-off could have been another important factor for the intensification of the trophic levels and the consequent instauration of a full Bryonoderm mode, especially with regard to land-attached carbonate depositional systems as the Finnmark Platform, where clastic input is an ordinary aspect. In the studied sections, but also in the coeval intervals of the shallow cores and in the underlying Gzhelian Ørn Formation (well 7128/6-1), a discrete amount of scattered quartz grains is always present (Bugge et al., 1995; Ehrenberg et al., 1998a); but a considerable relative increase of quartz-dominated very fine sand and silt is observed in the bryozoan-crinoidal wackestone-packstones (LA9) of the Ørn and the Isbjørn Formation. The clastic component within these intervals could likely reflect phases of increased land-derived siliciclastic supply associated with coastline retrogradation (Ehrenberg et al., 2000) and successive reworking due open circulation. However, in our case the observed increasing rate of insoluble detrital load could be an artifact due to burial compaction/dissolution, whose sedimentary features (stylolites and nodular seams) represent a typical aspect of the lithofacies association LA9.

The Finnmark Platform large scale geometries

641 The Finnmark area is affected by the Late Devonian–middle Carboniferous inherited extensional trend
642 (reactivated following the Caledonian structures), striking NE-SW and marking the overall boundary
643 with the Nordkapp Basin (Faleide et al., 1984; Gudlaugsson et al., 1998). Prior to the deposition of the
644 Ørn Formation, syn-rift structural highs were eroded and the depressions partially filled by clastics of
645 the Billefjorden and "lower" Gipsdalen Group (Ugle and Falk Formation). Therefore, following the
646 Moscovian transgression, the onset of the Ørn Formation carbonates on the Finnmark Platform took
647 place in relatively diverse and subsiding neritic settings reflecting local physiography, along with the
648 previous-mentioned climatic and oceanographic changes. This makes not straightforward to assess how
649 the large scale depositional profile of the platform evolved following the biological shift between the
650 Gipsdalen and Bjarmeland Group, and how to classify this system according with the current geometric
651 classifications that vary from rimmed shelves and homoclinal ramps, through a wide number of
652 transitional profiles (Pomar, 2001; Williams et al., 2011). Such complexity is also revealed by the
653 dissimilar hypotheses made by previous authors (on the base of seismic- and/or core analyses) about the
654 development of the platform profile across the Gipsdalen-Bjarmeland transition.
655 For example, Nilsen et al. (1993) considered a major shift from a homoclinal ramp during the
656 deposition of the Gipsdalen Group to a rimmed shelf with marginal buildups during the deposition of
657 Bjarmeland Group, whereas Ehrenberg et al., (1998a) suggested that a ramp profile (with a marginal
658 buildup trend) was already established during the deposition of the Gipsdalen Group". Later, Colpaert et
659 al. (2007) suggested a shift from a prograding carbonate platform/slope system with marginal buildup
660 complexes during the deposition of the Gipsdalen Group, to a restricted heterozoan platform with
661 stacked buildup complexes on the slope during the deposition of the Bjarmeland Group. Finally,
662 Rafaelsen et al. (2008) suggested that the Finnmark was a "northerly dipping distally steepened ramp
663 with buildups" from the mid Carboniferous throughout the Permian, with detached intra-basinal

664 platforms (structural high on well site 7229/11-1) that became attached to the ramp during the deposition
665 of the transgressive Bjarmeland Group.
666 A generally accepted feature, in all the studies, is represented by an arched-like platform margin active
667 during the deposition of the Gipsdalen Group, revealed by seismic profiles and partially controlled by
668 the inherited NW-SE lineaments. The E-W trend of the margin and its approximate position across the
669 platform (fig. 9a) is given by considering the southern depositional limit of the Gzhelian–Asselian
670 lowstand evaporitic sequences of the Nordkapp Basin, pinching out on the margin itself (Gérard and
671 Buhrig, 1990; Bruce & Toomey 1993; Gudlaugsson et al., 1998; Ehrenberg et al., 1998a; Colpaert et al.,
672 2007). Similarly, the overall distribution of the late Sakmarian–Artinskian heterozoan buildups of the
673 Polarrev Formation (Bjarmeland Group) has been seismically mapped within the Finnmark domain
674 (Gudlaugsson et al., 1998; Ehrenberg et al., 1998a). Their southern limit is mostly placed slightly basin-
675 ward of the Gzhelian–Asselian basinal evaporites and follow nearly the same lineaments along the
676 platform (fig. 9b).
677 On the base of these assumptions, we propose that the key to delineate a reliable development of the
678 Finnmark Platform depositional profile through time, together with the information from the facies
679 analyses, could be given by considering i): the location of the buildups across the platform, their
680 forming-biota and shape variation across the Gipsdalen and Bjarmeland Groups; ii) the position of the
681 margin and its evolution in terms of depth and morphology. These points have certainly a strong
682 implication on assessing the geometry of the Finnmark Platform because, according with the classical
683 models of the carbonate sedimentology, a shallow marginal barrier would point to a more flat-topped
684 platform whereas an offshore deeper margin to a distally steepened ramp profile (Read, 1985; Pomar,
685 2001 and references therein).

686 Previous and current cores analyses from the wells 7128/6-1, 7128/4-1 and shallow cores (Bugge et al.,
687 1995; Ehrenberg et al., 1998a; Ehrenberg et al. 2000) have assessed that the deposition of the Ørn
688 Formation in the proximal platform areas were characterized by presence of scattered (up to 6m) bio-
689 constructions dominated by *Palaeoaplysina*-phylloid algae and subordinate corals. These bodies likely
690 had a tabular and laterally extended (>100 m-wide) morphology, as has been highlighted by multi-
691 attribute analyses in the proximal areas of the 3D cube ST9802 (Colpaert et al., 2007; fig. 1b for
692 location). Cyclic subaerial exposures bounding the buildup bodies in the proximal domains suggest the
693 reduced accommodation space as the main factors limiting their vertical growth, favoring in turn their
694 lateral development (Stemmerik et al., 1999; Colpaert et al., 2007). On the other hand, seismic-scale
695 mounded features within the Ørn Formation have been interpreted as buildups along the marginal
696 domains of platforms and structural highs (Samuelsberg et al., 2003; Colpaert et al., 2007; Rafaelsen et
697 al., 2008), even though a precise assessment of the biota making these buildups is strongly limited by
698 missing cored sequences through the observed mounded features.
699 An example of marginal bioconstructions developing on a seismic scale during the deposition of the
700 Gipsdalen Gp has been shown in the distal part of the 3D seismic cube ST9802 (Colpaert et al. 2007),
701 where Asselian seismic scale mounded structures have been interpreted as transgressive/highstand
702 polygonal buildup complexes (top SU2, Base Asselian Horizon), as well as km-long complex (top SU3,
703 below the UAH) associated to a platform barrier. According to this interpretation, starting from the early
704 Asselian (SU2-SU3 seismic units, see fig. 3) the system evolved as a rimmed platform with a prograding
705 margin and a slope (up to 400 m-high), on which the lowstand basinal evaporites pinched out. Later, on
706 top of the Mid Sakmarian Horizon (MSH), the transgressive sequence corresponding to the lower part of
707 the Bjarmeland Gp (fig. 3) led to retrogradation of the margin and the development of a restricted
708 heterozoan platform with stacked bryozoan-*Tubiphytes* buildup complexes on the slope.

In this study, the 2D seismic sequence stratigraphic interpretation of the marginal platform area (fig. 10b) shows, similarly to Colpaert et al. (2007), a carbonate system prograding during highstand phases of the third-order depositional sequences S-3 and S-4, bounded by MGH, UAH and MSH. Seismic--scale mounded buildup-like morphologies are also recognized on the margin and the slope areas between MGH and UAH (fig. 10b).

With the available data it is not possible to assess the nature of the biotic associations making up the marginal buildups associated with the Ørn Formation, which would mainly depend on the dominant palaeoecological settings favoring certain reef-builders more than others. It has been suggested that also the marginal and distal/deeper buildup assemblages were dominated by *Palaeoaplysina* and phylloid algae associations, assimilated to the outcropping stacked complex observed in the Kapp Dunér Formation in Bjørnøya (Lønøy, 1988; Stemmerik et al., 1994; Stemmerik and Worsley, 2005). However, according with the facies study proposed here, during the deposition of the Ørn Formation the Finnmark offshore environments were characterized by heterozoan assemblages (fig. 8); therefore we cannot exclude that deep bryozoan-*Tubiphytes* buildups/mounds developed on the Finnmark platform also during the Gzhelian-Asselian time, prior to the formation of the facies-equivalent and much thicker (Colpaert et al., 2007; Rafaelsen et al., 2008) overlying complexes of the Bjarmeland Group (described in the distal well 7229/11-1).

This possibility is further supported by the light-dependent nature of the *Palaeoaplysina*-phylloid algae buildups and their frequent associated fauna, commonly thriving in the shallowest platform domains (inner to middle ramps). Similarly, a depth-related change in biotic buildups composition at tropical-subtropical latitudes, from the shallow *Palaeoaplysina*-phylloid algae to the deeper bryozoan-dominated buildups has been observed during the Asselian-Sakmarian of the Sverdrup Basin (Beauchamp, 1993; Beauchamp and Desrochers, 1997) and during the early Carboniferous (Moscovian) of the north

732 Greenland (Stemmerik, 2003). In the latter, buildups dominated by bryozoans and associated heterozoan
733 fauna have been placed around the lower limit of the photic zone.
734 Hence, on the base of these assumption and from the large-scale view of the seismic line of fig. 10a, we
735 suggest to consider the eastern Finnmark Platform geometry during the deposition of the Ørn Formation
736 as a wide (>100km) distally steepened ramp (fig. 10a). We believe that the carbonate system was gently
737 grading toward the offshore domains where a subtidal margin/slope system (below the SWB) was
738 associated with the development of seismic scale heterozoan-dominated buildups during transgressive–
739 highstand phases (fig. 10c), favored by accommodation rates (due to the coupled effect of eustacy and
740 subsidence rates) greater than in most of the proximal areas of the platform.
741 Hence, it can be assumed that during the deposition of the Ørn Formation, while the shallowest ramp
742 domains were dominated by peritidal m-scale cycles capped by subaerial exposures and possible
743 formation of structurally-controlled late highstand-lowstand evaporitic deposits (Samuelsberg et al.,
744 2003), the distal depositional areas were mostly sites of subtidal cyclicity and more open circulation.
745 Similarly, Stemmerik (2008) affirms that on the Finnmark domain and during the deposition of the Ørn
746 Formation: “most deposition seems to have taken place in deeper-water, mid- and outer-shelf
747 environments”. In fact, contrarily to what is observed in the proximal domains, the stacked nature of the
748 distal buildups forming seismically recognizable features should clearly point to the presence of a
749 greater available space during transgressive and early highstand phases.
750 Later, with the deposition of the Bjarmeland Gp and the instauration of the Bryonoderm sedimentation
751 mode, heterozoan buildups developed almost across the whole ramp. In the most proximal domains, the
752 presence of heterozoan bio-constructions below the seismic resolution cannot be excluded. However,
753 they have not been observed, nor in the cored intervals of the well 7128/6-1 (fig. 3) neither in the coeval
754 shallow cores (Ehrenberg et al. 2000). In the distal shelf areas close to the margin, composition and

755 shape of the heterozoan buildup complexes of the Polarrev Formation are well known from the well
756 7229/11-1 (Blendinger et al., 1997; Stemmerik, 1997) and from detailed 3D seismic interpretations
757 (Rafaelsen et al. 2008; Colpaert et al. 2007). They are dominated by bryozoan-*Tubiphytes* framestones
758 and stromatactis mud-wackestones forming mounds and ridges of 350–1500 m-wide, more than 27 km-
759 long and up to 325 m-high. Their approximate trend along the Finnmark Platform is shown in figure 9.
760 The seismic interpretation of the line 213, also supported by the interpretation of Colpaert et al. (2007)
761 shows that the heterozoan buildups complexes of the Polarrev Formation developed between MSH and
762 BKH in a slightly distal position with respect to the offshore margin of the underlying prograding
763 distally steepened ramp (see fig. 9). Onlap reflectors on top of MSH are associated with the major
764 transgressive Sakmarian depositional phase of the Bjarmeland Group, causing the stepwise reduction of
765 the pre-existent slope gradient (fig. 10b-c). Therefore, we suggest that the shift to the Bjarmeland Group
766 possibly led to the instauration of a heterozoan-dominated homoclinal ramp, devoid of a clear subtidal
767 margin/slope system and gently grading toward the Nordkapp Basin. Huge heterozoan buildup
768 complexes developed in the outer ramp, growing on the seafloor and along topographic/structural reliefs
769 as isolated mounds and polygonal ridges and supported by optimal ecological conditions, coupled with
770 the available accommodation space created by tectonic subsidence and eustatic sea-level rise. In fact,
771 after the Sakmarian major flooding and according with the current palaeoceanographic/palaeoclimatic
772 scenario, the increased accommodation, lowering of the seawater temperatures and enhanced trophic
773 levels created the best conditions for the heterozoan biota to create the observed mounded belt across the
774 offshore late Sakmarian–late Asselian Finnmark environments (fig. 10b-c).

775

776 **Implications from hydrocarbon perspective**

777 The described interplay between climatic/oceanographic/geodynamic factors across the Upper
778 Carboniferous-Lower Permian and the resulting major biotic turnover and large scale geometries
779 strongly influenced the depositional history of the Finnmark Platform with major influences on the
780 development of potential Palaeozoic plays in the areas. Core-based reservoir models and diagenetic
781 studies (Ehrenberg et al., 1998b; Stemmerik, 1999) from the well 7128/6-1 indicate that the Ørn
782 Formation is characterized by many high (primary and secondary) porosity intervals, given by a
783 combination of different favorable factors as dolomitization and meteoric leaching of the metastable
784 aragonitic skeletals, associated with high amplitude/frequency sea-level fluctuations. Such features led
785 considering the Chloroforam shallow domains and the *Palaeoaplysina*-phylloid buildups of the
786 Gipsdalen Gp as the best potential reservoirs of the Barents Sea area (Stemmerik, 1999; Stemmerik and
787 Worsley, 2005). On the other hand, the subtidal Isbjørn Formation carbonates and buildup complexes
788 show very low porosities and are considered non-prospective, due to the overall stable mineralogy of its
789 biotic components (low-Mg calcite) and the common presence of silty-clayey horizons favoring
790 dissolution and calcite cementation through stylolites. Assuming the shelf profile as a distally steepened
791 ramp rather than a flat-topped platform during the deposition of the Ørn Formation, as our data suggest,
792 has dramatic implications for reservoir studies. In fact the lateral extension of the areas affected by
793 subaerial exposure on the shelf (more prone to develop secondary porosity) and therefore more
794 prospective in terms of potential reservoir interval, change drastically according with the two different
795 scenarios. This represents a key point to take in account when planning future exploration in the eastern
796 Finnmark domains and in other buried land-attached Palaeozoic carbonate depositional systems along
797 the Arctic epicontinental shelf.
798
799 Figure 9 here

Figure 10 here, full page

Conclusions

- Facies analysis of the uppermost Ørn Formation from the cores 7128/6-1 and 7128/4-1 of the Finnmark Platform reveals that during the Asselian–early Sakmarian the shallowest inner ramp environments were dominated by a Chloroforam sedimentation mode and photozoan biota. Such communities were laterally replaced, towards the deeper and distal outer ramp environments, by mixed Bryonoderm-extended and by heterozoan Bryonoderm assemblages. In view of this depth-related transition in carbonate factories, and according with the coeval palaeoceanographic-palaeoclimatic scenario across the Arctic domain (sub-/tropical latitudes of deposition, open connection and current circulation with the Tethyan tropical realm), our results support the hypothesis of the presence of a stratified water column and a thermocline separating the photozoan biota thriving in shallow and warm waters from the heterozoan associations, well adapted to deeper and cooler mesotrophic waters.

- The shift from the Ørn to the Isbjørn Formation in the proximal well 7128/6-1 reveals the full instauration of the Bryonoderm sedimentation mode on the Finnmark Platform, starting from the middle-late Sakmarian. Transgressive heterozoan facies invaded also the proximal shallow shelf areas (before occupied by photozoan communities) favoring the installation of an open and storm-dominated ramp. Such modifications of the depositional style in favor of the heterozoan communities were driven by the evolution of climatic-oceanographic Arctic scenario (melting phases of the Gondwanan icecaps, cooling due to drifting to temperate latitudes, closure of the

823 connections with the Tethyan realm) that led to the disruption of the thermocline with
824 consequent influx of nutrient-rich cool waters across the Finnmark domain.
825
826 • Our facies and palaeoenvironmental analysis (supported by 3D seismic interpretations), suggest
827 that during the deposition of the Ørn Formation, *Palaeoaplysina*, phylloid algae and rugose
828 corals were responsible for the formation of m-scale buildup patches within the inner to middle
829 ramp environments, whereas the still unexplored mounded seismic features observed offshore,
830 along the subtidal margin/slope system of the distally steepened ramp, could have been formed
831 by the heterozoan communities, according to the observed depth-related shift from chloroforam
832 to bryonoderm sedimentation mode. Following the middle Sakmarian transgression and the shift
833 to a heterozoan homoclinal ramp profile, bryozoan-*Tubiphytes* stacked buildup complexes
834 developed along the outer ramp domains.
835
836 • Our seismic interpretation across the eastern platform profile, coupled with facies and
837 palaeoenvironmental analysis, suggests that the eastern Finnmark large scale geometry changed
838 from a distally steepened ramp to homoclinal ramp, following the ongoing climatic-
839 oceanographic modifications and the consequent shift between the two major depositional phases
840 represented by the Gipsdalen and the Bjarmeland Groups. Due to the presence of high
841 frequency/amplitude glacio-eustatic fluctuations, it can be assumed that during the deposition of
842 the Gipsdalen Group the proximal ramp domains were cyclically subaerially exposed, whereas in
843 the outer ramp a subtidal cyclicity was more persistent. At the same time, major phases of
844 restriction and isolation of the Nordkapp Basin led to the deposition of subtidal evaporitic
845 sequences, pinching out on the distally-steepened ramp slope.

- Given the good reservoir properties of the Gzhelian–Sakmarian Gipsdalen Group within the Finnmark depositional domain and the whole Norwegian Barents Sea area, the assessment of changes in the platform depositional profile as suggested in this study, through the observed regional shifts in sedimentation modes, represents a fundamental point to take in account for future exploration purposes, due to the impact it has on the reservoir properties.

REFERENCES CITED

Beauchamp, B., 1993, Carboniferous and Permian reefs of the Sverdrup Basin, Canadian Arctic islands, in: T. O. Vorren, E. Bergsager, Ø. A. Dahl-Stamnes, et al., eds., Arctic Geology and Petroleum Potential. Norwegian Petroleum Society Special Publication no. 2, p. 217–241.

Beauchamp, B., 1994, Permian climatic cooling in the Canadian Arctic, in G. D. Klein, ed., Pangea: Paleoclimate, Tectonics and Sedimentation during accretion, Zenith and Break-up of a Super-Continent: Boulder, Geological Society of America Special Paper, 288, p. 229–246.

Beauchamp, B., and A. Desrochers, 1997, Permian warm- to very cold-water carbonates and cherts in northwest Pangea, in N. P. James and J. A. D. Clarke, eds., Cool-water carbonates: SEPM Special Publication, v. 56, p. 327–347.

Blendinger, W., B. Bowlin, F. R. Zijp, G. Darke, and M. Ekroll, 1997, Carbonate buildup flank deposits: An example from the Permian (Barents Sea, northern Norway) challenges classical facies models: Sedimentary Geology, v. 112, p. 89–103.

869

870 Blomeier, D., C. Scheibner, and H. Forke, 2009, Facies arrangement and cyclostratigraphic architecture
871 of a shallow-marine, warm-water carbonate platform: the Late Carboniferous Ny Friesland Platform in
872 eastern Spitsbergen (Pyefjellet Beds, Wordiekammen Formation, Gipsdalen Group), Facies, v. 55, p.
873 291–324.

874

875 Blomeier**,** D., D. Carmohn, H. Forke, and C. Scheibner, 2011, Environmental change in the Early
876 Permian of Spitsbergen: from a warm-water carbonate platform (Gipshuken Formation) to a temperate,
877 mixed siliciclastic-carbonate ramp (Kapp Starostin Formation): Facies, v. 57, 493–523.

878

879 Bosence, D., 2005, A genetic classification of carbonate platforms based on their basinal and tectonic
880 settings in the Cenozoic: Sedimentary Geology, v. 175, 49–72.

881

882 Breuninger, R. H., Canter, K. L., and P. E. Isaacson, 1989, Pennsylvanian–Permian *Palaeoaplysina* and
883 algal buildups, Snaky Canyon Formation, East-Central Idaho, U.S.A., in H. H. J. Geldsetzer, N. P.
884 James, and G. E. Tebbutt, eds., Reefs, Canada and Adjacent Areas: Canadian Society of Petroleum
885 Geology, Memoir, 13, p. 631–637.

886

887 Bugge, T., G. Mangerud, G. Elvebakk, A. Mørk, I. Nilsson, S. Fanavoll, and J. O. Vigran, 1995, The
888 Upper Paleozoic succession on the Finnmark Platform, Barents Sea: Norsk Geologisk Tidsskrift, v. 75,
889 p. 3–30.

890

Bugge, T., G. Elvebakk, S. Fanavoll, G. Mangerund, M. Smelror, H. M. Weiss, J. Gjelberg, S. E. Kristensen, and K. Nilsen, 2002, Shallow stratigraphic drilling applied in hydrocarbon exploration of the Nordkapp Basin, Barents Sea: Marine and Petroleum Geology, v. 19, p. 13–37.

Butler, G.P., 1970, Holocene gypsum and anhydrite of the Abu Dhabi Sabkha, Trucial Coast: an alternative explanation of origin: Third Symposium on Salt, p. 120–152.

Cecchi, M., 1993, Carbonate sequence stratigraphy: application to the determination of play models in the Upper Palaeozoic of the Barents Sea, offshore northern Norway, in T.O. Vorren, E. Bergsager, Ø. A. Dahl-Stamnes, E. Holter, B. Johansen, E. Lie, and T. B. Lund, eds., Arctic Geology and Petroleum Potential: Norwegian Petroleum Society Special Publication, 2, 419–438.

Ciarapica, G., L. Passeri, and C. B. Schreiber, 1985, Una proposta di classificazione delle evaporiti solfatiche: Geologica Romana, v. 24, p. 219–232.

Colpaert, A., N. Pickard, J. Mienert, L. B. Henriksen, B. Rafaelsen, and K. Andreassen, 2007, 3D seismic analysis of an Upper Palaeozoic carbonate succession of the Eastern Finnmark Platform area, Norwegian Barents Sea: Sedimentary Geology, v. 197, p. 79–98.

Davies, G. R., 1971, A Permian hydrozoan mound Yukon Territory. Canadian Journal of Earth Sciences, v. 8, p. 973–988.

913 Davies, G. R., 1989, Lower Permian Palaeoaplysinid mound, northern Yukon, Canada, in H. H. J.
914 Geldsetzer, N. P. James, and G. E. Tebbutt, eds, Reefs, Canada and Adjacent Areas: Canadian Society
915 of Petroleum Geology, Memoir, 13, p. 638–642.
916
917 Ehrenberg, S. N., E. B. Nielsen, T. A. Svånå, and L. Stemmerik, 1998a, Depositional evolution of the
918 Finnmark carbonate platform, Barents Sea: results from wells 7128/6-1 and 7128/4-1: Norsk Geologisk
919 Tidsskrift, v. 78, p. 185–224.
920
921 Ehrenberg, S. N., E. B. Nielsen, T. R. Svånå, and L. Stemmerik, 1998b, Diagenesis and reservoir quality
922 of the Finnmark carbonate platform, Barents Sea: results from wells 7128/6-1 and 7128/4-1: Norsk
923 Geologisk Tidsskrift, v. 78, p. 225–252.
924
925 Ehrenberg, S. N., N. A. H. Pickard, T. R. Svånå, I. Nilsson, and V. I. Davydov, 2000, Sequence
926 Stratigraphy of the inner Finnmark carbonate platform (Upper Carboniferous-Permian), Barents Sea –
927 correlation between well 7128/6-1 and the shallow IKU cores: Norsk Geologisk Tidsskrift, v. 80, p.
928 129–162.
929
930 Ehrenberg, S. N., N. A. H. Pickard, L. B. Henriksen, T. A. Svånå, P. Gutteridge, and D. McDonald,
931 2001, A depositional and sequence stratigraphic model for cold-water, spiculitic strata based on the
932 Kapp Starostin Formation (Permian) of Spitsbergen and equivalent deposits from the Barents Sea:
933 AAPG Bulletin, v. 85, p. 2061–2087.
934

935 Ehrenberg, S. N., 2004, Factors controlling porosity in Upper Carboniferous–Lower Permian carbonate
936 strata of the Barents Sea: AAPG Bulletin, v. 88, p. 1653–1676.
937
938 Flügel, E., 2004, Microfacies of Carbonate Rocks, analysis, interpretation and application, Springer-
939 Verlag, Berlin Heidelberg, 976 p.
940
941 Fokin, P. A., A. M. Nikishin, and P. A. Ziegler, 2001, Peri-Uralian and Peri- Palaeo-Tethyan Rift
942 systems of the East European Craton, in P. A. Ziegler, W. Cavazza, A. H. F. Robertson, and S.
943 Crasquin-Soleau, eds., Peri-Tethys Memoir 6: Peri-Tethyan Rift/Wrench Basins and Passive Margins:
944 Memoires du Museum National d'Histoire Naturelle, 186, p. 347–368.
945
946 Forsythe, G. T. W., R. Wood, and J. A. D. Dickson, 2002, Mass spawning in ancient reef communities:
947 Evidence from Late Paleozoic Phylloid Algae: Palaios, v. 17, p. 615–621.
948
949 Gabrielsen, R. H., R. B. Færseth, L. N. Jensen, J. E. Kalheim, and F. Riis, 1990, Structural elements of
950 the Norwegian continental shelf. Part 1: The Barents Sea region: Norwegian Petroleum Directorate
951 Bulletin 6, 33 p.
952
953 Goldhammer, R. K., E. J. Oswald, and P. A. Dunn, 1991, Hierarchy of stratigraphic forcing: example
954 From Middle Pennsylvanian shelf carbonates of the Paradox basin, in E. K. Franseen, W. L. Watney, C.
955 G. Kendall, and W. Ross, eds., eds., Sedimentary modeling: Computer Simulations and Methods for
956 Improved Parameter Definition, Kansas Geological Survey Bulletin, v. 233, p. 361–413.
957

958 Golonka, J., and D. Ford, 2000, Pangean (Late Carboniferous-Middle Jurassic) paleoenvironment and
959 lithofacies: Palaeogeography, Palaeoclimatology, Palaeoecology, v. 161, p. 1–34.
960
961 Groves, J. R., and G. P. Wahlman, 1997, Biostratigraphy and evolution of Late Carboniferous and Early
962 Permian smaller foraminifers from the Barents Sea (offshore Arctic Norway): Journal of Paleontology,
963 v. 71, p. 758–779.
964
965 Gudlaugsson, S. T., J. I. Faleide, S. E. Johansen, and A. J. Breivik, 1998, Late Palaeozoic structural
966 development of the southwestern Barents Sea: Marine and Petroleum Geology, v. 15, p. 73–102.
967
968 Hüneke, H., M. Joachimski, W. Buggisch, and H. Lützner, 2001, Marine carbonate facies in response to
969 climate and nutrient level: the Upper Carboniferous and Permian of Central Spitsbergen (Svalbard),
970 Facies, v. 45, p. 93–136.
971
972 James, N. P., 1997, The cool-water carbonate depositional realm, in N. P. James and J. A. D. Clarke,
973 eds., Cool-water carbonates: SEPM Special Publication 56, p. 1–20.
974
975 Keilen, H. B., 1992, Lower Permian sedimentary sequences in Central Spitsbergen, Svalbard, in K.
976 Nakamura, ed., Investigations on the Upper Carboniferous-Upper Permian succession of West
977 Spitsbergen: Department of Geology and Mineralogy, Faculty of Sciences, Hokkaido University, Japan,
978 p. 127–134.
979

980 Koch, J. T., and T. D. Frank, 2011, The Pennsylvanian-Permian transition in the low-latitude carbonate
981 record and the onset of major Gondwanan glaciation: Palaeogeography, Palaeoclimatology,
982 Palaeoecology, v. 308, p. 362–372.
983
984 Krotov, P., 1888, Geological research on the western slope of Urals of Solikamsk and Cherdynsk, Trudy
985 Geologicheskago Komiteta, St-Petersburg, 6, p. 297–534 (in Russian).
986
987 Larssen, G. B., G. Elvebakk, L. B. Henriksen, S. E. Kristensen, I. Nilsson, T. J. Samuelsberg, T. A.
988 Svånå, L. Stemmerik, and D. Worsley, 2002, Upper Paleozoic lithostratigraphy of the Southern
989 Norwegian Barents Sea: Norwegian Petroleum Directorate Bulletin, 9, 76 p.
990
991 Larssen, G. B., G. Elvebakk, L. B. Henriksen, S. E. Kristensen, I. Nilsson, T. J. Samuelsberg, T. A.
992 Svånå, L. Stemmerik, D., and D. Worsley, 2005, Upper Palaeozoic lithostratigraphy of the southern part
993 of the Norwegian Barents Sea: Norges Geologiske Underøkelse Bulletin, 444, 43 p.
994
995 Lees, A., and A. T. Buller, 1972, Modern temperate-water and warm-water shelf carbonate sediments
996 contrasted: Marine Geology, v. 13, p. 67–73.
997
998 Lønøy, A. 1988: Environmental setting and diagenesis of Lower Permian *Palaeoaplysina* buildups and
999 associated sediments from Bjørnøya, Implications for exploration of the Barents Sea: Journal of
1000 Petroleum Geology, v. 11, p. 141–156.
1001

1002 Mangerud, G. 1994, Palynostratigraphy or the Permian and lowermost Triassic succession, Finnmark
1003 Platform, Barents Sea: Review of Palaeobotany and Palinology, v. 82, p. 317–349.
1004
1005 Morin, J., A. Desrochers, and B. Beauchamp, 1994, Facies analysis of Lower Permian platform
1006 carbonates, Sverdrup Basin, Canadian Arctic Archipelago: Facies, v. 31, p. 105–130.
1007
1008 Mutti, M., and P. Hallock, 2003, Carbonate systems along nutrient and temperature gradients: some
1009 sedimentological and geochemical constraints: International Journal of Earth Sciences (Geol Rundsch),
1010 v. 92, p. 465–475.
1011
1012 Nakazawa, T, K. Ueno, H. Kawahata, and M. Fujikawa, 2011, Gzhelian–Asselian Palaeoaplysina–
1013 microencruster reef community in the Taishaku and Akiyoshi limestones, SW Japan: Implications for
1014 Late Paleozoic reef evolution on mid-Panthalassan atolls, Palaeogeography, Palaeoclimatology,
1015 Palaeoecology, v. 310, p. 378–392.
1016
1017 Nelson, C. S., 1988a, An introductory perspective on non-tropical shelf carbonates, in Nelson, C. S., ed.,
1018 Non-Tropical Shelf Carbonates-Modern and Ancient, Sedimentary Geology, v. 60, p. 3–14
1019
1020 Nelson, C. S., 1988b, Non-tropical carbonate deposits on the modern New Zealand shelf, in Nelson, C.
1021 S., ed., Non-Tropical Shelf Carbonates-Modern and Ancient, Sedimentary Geology, v. 60, p. 71–94.
1022
1023
1024 Pomar, L., 2001, Types of carbonate platforms: a genetic approach: Basin Research, v. 3, p. 313–334.

Pomar, L., and C. G. St. C. Kendall, 2007, Architecture of carbonate platforms: a response to hydrodynamics and evolving ecology, in J. Lukasik, and A. Simo, eds., Controls on Carbonate Platform and Reef Development: SEPM Special Publication, 89, p. 187–216.

Rafaelsen, B., G. Elvebakk, K. Andreassen, L. Stemmerik, A. Colpaert, and T. J. Samuelsberg, 2008, From detached to attached carbonate buildup complexes - 3D seismic data from the upper Palaeozoic, Finnmark Platform, southwestern Barents Sea: Sedimentary Geology, v. 206, p. 17–32.

Read, J. F., 1985, Carbonate platform facies models: AAPG Bulletin, v. 69, p. 1–21.

Reid, C. M., N. P. James, B. Beauchamp, and T. K. Kyser, 2007, Faunal turnover and changing oceanography: Late Palaeozoic warm-to-cool water carbonates, Sverdrup Basin, Canadian Arctic Archipelago: Palaeogeography, Palaeoclimatology, Palaeoecology, v. 249, p. 128–159.

Samuelsberg, T. J., G. Elvebakk, and L. Stemmerik, 2003, Late Palaeozoic evolution of the Finnmark Platform, southern Norwegian Barents Sea: Norsk Geologisk Tidsskrift, v. 83, p. 351–362.

Schlager, W., 2003, Benthic carbonate factories of the Phanerozoic: International Journal of Earth Sciences (Geol Rundsch), v. 92, p. 445–464.

Scotese, C. R., and W. S. McKerrow, 1990, Revised world maps and introduction, in W. S. McKerrow, C. R. Scotese, eds., Palaeozoic Palaeogeography and Biogeography: Memoir Geological Society of

1048 London, p. 1–21.
1049
1050 Scotese, C. R., and R. P. Langford, 1995, Pangea and the palaeogeography of the Permian, in P. A.
1051 Scholle, T. M. Peryt, and D. S. Ulmer-Scholle, eds., The Permian of Northern Pangea. Volume 1:
1052 Paleogeography, Paleoclimates, Stratigraphy, Springer-Verlag, Berlin, p. 3–18.
1053
1054 Skaug, M., C. E. Dons, Ø. Lauritzen, and D. Worsley, 1982, Lower Permian *Palaeoaplysina* bioherms
1055 and associated sediments from central Spitsbergen: Polar Research, v. 2, p. 57–75.
1056
1057 Steel, R. J., , 1984, Svalbard's post-Caledonian strata – an atlas of sedimentational patterns and
1058 palaeogeographic evolution, in A. M. Spencer, E. Holter, S. O. Johnsen, A. Mørk, E. Nysæther, P.
1059 Songstad, and Å Spinnangr, eds, Petroleum Geology of the North European Margin: Norwegian
1060 Petroleum Society, Graham and Trotman, London, p. 109–135.
1061
1062 Stemmerik, L., and D. Worsley, 1989, Late Paleozoic sequence correlation, North Greenland and the
1063 Barents Shelf, in J. D. Collinson, ed., Correlation in Hydrocarbon exploration: Norwegian Petroleum
1064 Society, Graham and Trotman, London, p. 100–113.
1065
1066 Stemmerik, L., and G. B. Larssen, 1993, Diagenesis and porosity evolution of Lower Permian
1067 Palaeoaplysina build-ups, Bjørnøya: An example of diagenetic response to high frequency sea level
1068 fluctuations in an arid climate, in A. D. Horbury, and A. D. Robinson, eds., Diagenesis and basin
1069 development: AAPG Studies in Geology 36, p. 199–211.
1070

1071 Stemmerik, L., P. A. Larson, G. B. Larssen, A. Mørk, and B. T. Simonsen, 1994, Depositional evolution
1072 of Lower Permian Palaeoaplysina build-ups, Kapp Duner Formation, Bjørnøya, Arctic Norway:
1073 Sedimentary Geology, v. 92, p. 161–174.
1074
1075 Stemmerik, L., 1997, Permian (Artinskian–Kazanian) cool-water carbonates in North Greenland,
1076 Svalbard and the western Barents Sea, in N. P. James, and J. A. D. Clarke, eds., Cool-water carbonates,
1077 Society of Economic Paleontologists and Mineralogists Special Publication, 56, p. 349–364.
1078
1079 Stemmerik, L., G. Elvebakk, and D. Worsley, 1999, Upper Palaeozoic carbonate reservoirs on the
1080 Norwegian Arctic Shelf: delineation of reservoir models with application to the Loppa High: Petroleum
1081 Geoscience, vol. 5, p. 173–187.
1082
1083 Stemmerik, L., 2000, Late Palaeozoic evolution of the North Atlantic margin of Pangea:
1084 Palaeogeography, Palaeoclimatology, Palaeoecology, v. 161, p. 95–126.
1085
1086 Stemmerik, L., and D. Worsley, 2000, Upper Carboniferous cyclic shelf deposits, Kapp Kåre Formation,
1087 Bjørnøya, Svalbard: response to high frequency, high amplitude sea level fluctuations and local
1088 tectonism: Polar Research, v. 19, p. 227–249.
1089
1090 Stemmerik, L., 2003, Controls on localization and morphology of Moscovian (Late Carboniferous)
1091 carbonate buildups, southern Amdrup Land, North Greenland, in W. M. Ahr, P. M. Harris, W. A.
1092 Morgan, and I. D. Somerville, eds, Permo-Carboniferous Carbonate Platforms and Reefs. SEPM Special
1093 Publication no. 78, p. 253–265.

Stemmerik, L., and D. Worsley, 2005, 30 years on - Arctic Upper Paleozoic stratigraphy, depositional evolution and hydrocarbon prospectivity: Norwegian Journal of Geology, v. 85, p. 151–168.

Stemmerik L., 2008, Influence of late Paleozoic Gondwana glaciations on the depositional evolution of the northern Pangean shelf, North Greenland, Svalbard, and the Barents Sea, in C. R. Fielding, T. D. Frank, and J. L. Isbell, eds., Resolving the Late Paleozoic Ice Age in Time and Space: Geological Society of America Special Publication, 441, p. 205–217.

Stuckenberg, A. A., 1895, Korally I Mshanki Kammennouolnykh otlozhenii Urala I Timana: Trudy Geologicheskago Komiteta, 10, 178 p.

Tucker, M. E., and V. P. Wright, 1990, Carbonate sedimentology: Blackwell, Oxford, 496 p.

Vachard, D., and P. Kabanov, 2007, *Palaeoaplysina* gen. nov. and *Likinia* Ivanova and Ilkhobskii, 1973 emend., from the type Moscovian (Russia) and the algal affinities of the ancestral palaeoaplysinaceae n. comb.: Geobios, v. 40, p. 849–860.

Wahlman, G. P., 2002, Upper Carboniferous–Lower Permian (Bashkirian–Kungurian) mounds and reefs, in W. Kiessling, E. Flügel, and J. Golonka, eds., Phanerozoic Reef Patterns: SEPM Special Publication, 72, p. 271–338.

1116 Warren, J. K, 2006, Evaporites: Sediments, Resources and Hydrocarbons, Springer-Verlag, Berlin, 1036
1117 p.
1118
1119 Williams, H. D., P. M. Burgess, V. P. Wright, G. Della Porta, and D. Granjeon, 2011, Investigating
1120 carbonate platform types: multiple controls and a continuum of geometries: Journal of Sedimentary
1121 Research, v. 81, p. 18–37.
1122
1123 Worsley, D., T. Agdestein, J. Gjelberg, K. Kirkemo, A. Mørk, I. Nilsson, S. Olaussen, R. J. Steel, and L.
1124 Stemmerik, 2001, The geological evolution of Bjørnøya, Artic Norway: implications for the Barents
1125 Shelf: Norwegian Journal of Geology, v. 81, p. 195–234.
1126
1127 Worsley, D., 2006, The post-Caledonian geological development of Svalbard and the Barents Sea:
1128 Norsk Geologisk Forening, Abstracts and Proceedings, no. 3.
1129
1130 Wright, V. P., and T. P. Burchette, 1996, Carbonate ramps: an introduction, in V. P. Wright, and T. P.
1131 Burchette, eds., Carbonate Ramps, Geological Society of London, Special Publication, v. 149, p. 1–5.
1132
1133 Wright, V. P., and T. P. Burchette, 1996, Shallow-water carbonate environments, in H. G. Reading, ed.,
1134 Sedimentary Environments: Processes, Facies and Stratigraphy, Blackwell Science Ltd, Oxford, p. 325–
1135 394.

Facies and seismic analysis of the Late Carboniferous–Early Permian Finnmark carbonate Platform (southern Norwegian Barents Sea): an assessment of the carbonate factories and depositional geometries.

Figure captions

Figure 1. a) Late Pennsylvanian (Gzhelian stage, 300 Ma) palaeoceanographic map (from http://cpgeosystems.com/globaltext2.html) and palaeo-position of the Finnmark Platform domain within the Arctic epicontinental shelf. b) Structural/depositional domains of the Norwegian Barents Sea. The Finnmark Platform, object of this study, is bordered by the Norwegian land to the south and by the Nordkapp Basin to the north. The map shows the position of the four exploration wells reaching the Palaeozoic interval and the three shallow exploration cores mentioned in the text. The position of the selected 2D seismic line ST9715-213 across the NE-SW platform profile (fig. 8) is shown, together with the 3D cube ST9802. HB: Hammerfest Basin; HBS: Harstad Basin; NH: Norsel High; SD: Samson Dome; ND Nordvang Dome. Modified after Samuelsberg et al (2003).

Figure 2. Late Palaeozoic Lithostratigraphic Units of the Southern Norwegian Barents Sea and their relationship across the Finnmark Platform profile (Modified after Larssen et al., 2005). The stratigraphic intervals of the studied wells 7128/6-1 and 7128/4-1 of the Gipsdalen Gp (Ørn Formation) and the Bjarmeland Gp (Isbjørn Formation) are also shown.

Figure 3. Stratigraphic correlation between the wells 7128/6-1 and 7128/4-1 across the Gipsdalen, Bjarmeland and Tempelfjorden Groups. The scheme is based on the integration of GR profiles, 2nd and 3rd order (S-1 to S-7) depositional sequences, Lithostratigraphic Units (L1 to L-9 (from Ehrenberg et al.,

1998a) and fusulinid-based biostratigraphy (Ehrenberg et al., 2000). Seismic horizons (dashed lines) and related seismic units (SU1–SU6) across the well 7128/6-1 are from Colpaert et al. (2007). MCH: middle Carboniferous Horizon UCH: upper Carboniferous Horizon, MGH: middle Gzhelian Horizon, BAH: base Asselian Horizon, UAH: upper Asselian Horizon, MSH: middle Sakmarian Horizon, BKH: base Kungurian Horizon, BKH: base Tatarian Horizon. The blue-colored horizons are the ones considered for this study (MCH, MGH, UAH, MSH, and BKH) and represented as blue-dashed lines. Dark green segments correspond to the intervals investigated for this study.

Figure 4. Logs showing the main lithological, stratigraphic and sedimentological features of the studied Asselian-Artinskian intervals from the wells 7128/4-1 (log 1) and 7128/6-1 (logs 2 and 3). For an easier overview of the figure, the stratigraphic relationship between the logs is also shown in the small, pink rectangle. Refer to the text for the explanation of the Lithofacies associations (LA) and their evolution/changes through the sections. Textures/lithologies: c: clay; m/e: mudstone/evaporite; w: wackestone; fs: fine sandstone; p: packstone; g: grainstone; b: boundstone.

Figure 5. Core pictures from the Asselian-Artinskian studied interval, of some of the lithofacies associations (LA) described in the text. a) Densely packed mm to cm anhydrite nodules in a dolomitic/silty matrix (LA1) from the Ørn Formation interval of the well 7128/4-1 (1839.5m). b) Particular of *Palaeoaplysina* boundstones (LA6a) from the Ørn Formation interval of the well 7128/4-1 (1818.4m). Note the horizontal/mounded arrangement of the *Palaeoaplysina* plates (p) and the muddy matrix (m) occasionally trapped in the interplate space during successive phases of buildup development. Note also the typical protuberances of the *Palaeoaplysina* thallus (arrows, See also the thin section photograph in plate 3a). c) Particular of coral boundstones (LA6b) from the Ørn Formation

interval of the well 7128/6-1 (1843.4m). The colony of rugose corals shows a cerioid arrangement of the corallites, forming a massive framework. d) Rugose coral boundstones (LA6b) from the Ørn Formation interval of the well 7128/6-1 (1839.4m). The colony shows a phaceloid growth type of the corallites, surrounded by bioclastic grainstones of the lithofacies association LA5. e) Erosive surface marking the stratigraphic boundary between the Gipsdalen Gp and the Bjarmeland Gp in the well 7128/6-1 (1834.7m). Shallow bioclastic grainstones (LA5) of the Ørn Formation, reflecting a Chloroforam sedimentation mode, are cut by an erosive surface and overlied by about 5cm of nodular siltstone, passing upward to subtidal crinoidal-bryozoan grainstones (LA8) of the Isbjørn Formation, associated to a Bryonoderm sedimentation mode. See the text for further explanation.
f) Outer ramp crinoidal-bryozoan silty wackestone-packstones (LA9) from the Isbjørn Formation interval of the well 7128/6-1 (1813.8m). The pseudo-nodular aspect of this LA is mostly due to the dissolution of the calcareous component during burial compaction, associated with high silt/clay content.

Figure 6. Thin sections photographs of the most representative lithofacies associations (LA).
a) Dolomitized mudstones (LA2) from the Ørn Formation interval of the well 7128/4-1 (1853m). The microfacies shows mm-sized cavities possibly related to intertidal fenestrae or birdseyes, filled by anhydrite cement in a fine dolomitic/micritic matrix, with high intercrystalline porosity. b) Fine quartzose-calcareous sandstones (LA3) from the Ørn Formation interval of the well 7128/4-1 (1814m). The carbonate content is characterized by skeletal fragments (up to 30 %) and in minor amount by blocky calcitic spar. The microfacies shows a high interparticle porosity. c-d) Bioclastic wackestone-packestones (LA4) from the Ørn Formation interval of the well 7128/4-1 (1815m and 1842m respectively) showing calcareous algae (*Epistomora sp.*, E), benthic foraminifera (F) encrustations of bryozoans (B), *Tubiphytes* (T) and possible *Girvanella* (G). No visible porosity e) Bioclastic grainstones

(LA5) from the Ørn Formation interval of the well 7128/4-1 (1865m) dominated by globivalvulinid foraminifera (Gv) and peloids, plus undifferentiated recrystallized skeletal fragments and encrusting forms. f) Bioclastic grainstones (LA5) from the well 7128/6-1 (1837.75m) dominated by red algae (*Komia* sp.) (K), bryozoan fragments and peloids. Note also the well developed interparticle-moldic porosity. g) Rugose coral boundstones (LA6b) from the Ørn Formation interval of the well 7128/4-1 (1849.25m). The picture shows a micropeloidal matrix (m) and different generations of calcitic (c) and anhydrite (a) cements, partially filling intergranular, intragranular and moldic/vuggy pores. Note the high intraparticle porosity within the corallites. h) Bioclastic packstones (with dolomitized matrix) occupying the interstitial space of the coral boundstones (LA6b), from the Ørn Formation interval of the well 7128/4-1 (1849.25m). It shows coral and crinoid fragments plus others undifferentiated skeletal components, often encrusted by *Girvanella* (G); *Tetrataxis* (Tx) and *Tuberitina* (t) foraminifera can be recognized. Note also the high interparticle-moldic porosity.

Figure 7. Thin sections photographs of the most representative lithofacies associations (LA).

a-b) *Palaeoaplysina* boundstones (a) (LA6a) and interstitial matrix (b) (LA4) from the Ørn Formation interval of the well 7128/4-1 (1818 m). The thallus morphology of *Palaeoaplysina* shows the typical protuberances (p) and the upward-branching tubes (t) of the canal system mostly filled by the interstitial matrix. The latter is made by bioclastic packstones from LA4, showing small benthic foraminifera (F), fine fragments cystoporid bryozoans (B), ostracods (O) and possible *Tubiphytes* (T), plus undifferentiated recrystallized skeletal grains.

c-d) Foraminiferal packstones (LA7) from the Ørn Formation interval of the well 7128/4-1 (1837m). The microfacies is dominated by fusulinid foraminifera (F), with fragments of crinoids (C) and *Rugose* corals (R), less small benthic foraminifera. In photo (d) the microfacies reflects a probable more distal

93 position. It shows scattered fusulinids (F) and *Tetrataxis* (Tx) foraminifera, crinoid (C) and trilobite (Tr)
94 fragments, plus other undifferentiated shells. The matrix is partially dolomitized, including common
95 sparse quartz grains (Ørn Formation interval of the well 7128/4-1, 1864 m).
96 e) Crinoidal-bryozoan grainstones (LA8) from the Ørn Formation interval of the well 7128/4-1 (1824m).
97 The microfacies is dominated by fragments of crinoids (C) and bryozoans (B). It shows moderate
98 interparticle-intraparticle porosity when pores are not occluded by syntaxial overgrowth of calcitic
99 cement.
100 f) Crinoidal-bryozoan grainstones (LA8) from the Isbjørn Formation interval of the well 7128/6-1
101 (1809.75m). It is characterized by fragments of crinoids (C), bryozoans (B) and *Tubiphytes* (T). The
102 microfacies is very similar to the one observed within the Ørn Formation (photo e) but in this case, as
103 for the whole the Isbjørn Formation interval studied, the porosity is very low, due to complete occlusion
104 by syntaxial and blocky cements.
105 g-h) Crinoidal-bryozoan silty wackestone-packstones (LA9) from the Ørn Formation interval of the well
106 7128/4-1 (1825 m). The microfacies shows chaotically arranged fragments of crinoids (C) and
107 bryozoans (B) in a calcisiltitic matrix with abundant quartz grains. In the more distal wackestones (photo
108 h) the grain-size decreases and the amount of matrix increase.
109
110 **Figure 8**. Schematic depositional models derived from the Asselian-Artinskian intervals of the wells
111 7128/6-1 and 7128/4-1, during the deposition of (a) the Ørn Formation (Gipsdalen Gp) and (b) the
112 Isbjørn Formation (Bjarmeland Gp). The models show the interpreted platform sub-environments, the
113 spatial distribution of the Lithofacies Associations (LA1-LA9) the relative abundance of the major
114 skeletal components across the platform profile and water masses circulation according with the shift in

carbonate sedimentation modes, driven by major changes in the palaeoceanographic/palaeoclimatic conditions (see text for explanation). See figure 4 for the color code of the LA.

Figure 9. a) Gzhelian-Asselian large-scale facies map showing the limit of the subtidal evaporites of the Nordkapp Basin (sulphatic evaporites and halite sequences cored from the wells 7228/9-1 S and 7229/11-1). The southern limit (contour in green) marks the approximate position of the palaeo-margin at the Finnmark Platform/Nordkapp Basin transition. B) Sakmarian–Artinskian large scale facies map of the Finnmark domain showing the seismically-interpreted large-scale distribution of the Sakmarian-Artinskian stacked heterozoan buildup complexes. Modified after Gudlaugsson et al. (1998).

Figure 10. Seismic interpretation of the 2D line ST9715-213. a) Large scale view of the seismic line across the SE-NW profile of the eastern Finnmark Platform and the seismic intervals corresponding to the entire Gipsdalen Gp and Bjarmeland Gp. The line covers approximately 97 km in length. b) Seismic profile showing the five selected horizons discussed in the text (in yellow) and the top Permian horizon (in white), across the marginal platform area. c) Interpreted seismic profile derived from b, showing the evolution of the marginal part of the Finnmark platform across the Gipsdalen and Bjarmeland Gp transition. Note the change in geometries of the reflectors/margin, interpreted as associated to a change from a distally steepened ramp (Ørn Formation) to homoclinal ramp (Bjarmeland Gp) profile. See text for the detailed discussion.

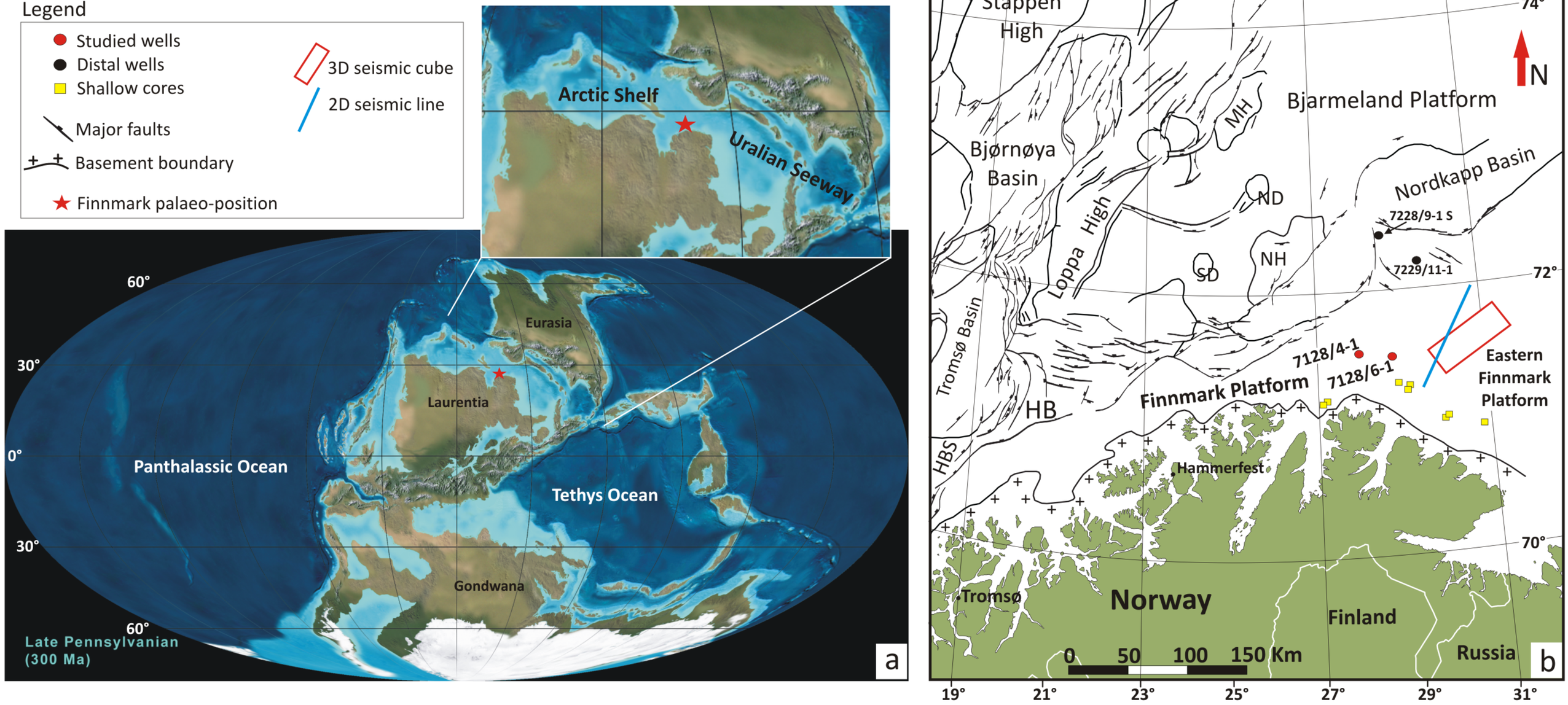
Legend
Studied wells
Distal wells
Shallow cores
Major faults
Basement boundary
Finnmark palaeo-position
3D seismic cube
2D seismic line
Arctic Shelf
Uralian Seeway
60°
30°
0°
30°
60°
Eurasia
Laurentia
Panthalassic Ocean
Tethys Ocean
Gondwana
Late Pennsylvanian
(300 Ma)
a
Stappen
High
74°
N
Bjarmeland Platform
MH
Bjørnøya
Basin
Loppa High
ND
Nordkapp Basin
7228/9-1 S
7229/11-1
SD
NH
72°
Tromsø Basin
7128/4-1
7128/6-1
Eastern
Finnmark
Platform
Finnmark Platform
HB
HBS
Hammerfest
70°
Tromsø
Norway
Finland
Russia
0 50 100 150 Km
b
19°
21°
23°
25°
27°
29°
31°

Period/Epoch | Gp | Formation | Finnmark (Basinward / Landward) | Studied Intervals

Permian

Early

Lopingian

Guadalupian

Kungurian

Artinskian

Sakmarian

Asselian

Carboniferous

Late

Gzhelian

Kasimovian

Moscovian

Bashkirian

Early

Serpukhovian

Viséan

Tournasian

Tempelfjorden

Bjarmeland

Gipsdalen

Billefjorden

?

Ørret

Røye

?

Isbjørn

Ulv

Polarrev

Ørn

Falk

Ugle

Blaererot

Tettegras

Soldogg

7128/6-1

7128/4-1

Conglomerates

Sandstones

Shales

Coal

Dolomitic limestones/dolostones

Limestones

Halite

Anhydrite

Chert

Carbonate buildups

Well 7128/4-1

Gp (Fm)

Depositional sequences
Ehrenb. et al. (1998a)

MD (m)

Gamma Ray
20 60 100 140

Tempelfjorden Gp (Røye Fm)

Bjarmeland Gp
Isbjørn Fm

Gipsdalen Gp (Ørn Fm)

S-4

1600
1700
1800
1900
2000

Lithostratigraphic Units
Ehrenberg et al. (1998a)

L-9
Offshore shaly limestones, spiculitic limestones and spiculites

L-8
Open shelf limestones and shaly limestones

L-7
Shallow subtidal limestones and transgressive open shelf shaly limestones

L-6

L-5
Intertidal dolomitic limestones

L-4
Subtidal buildup-dominated limestones

L-3
Intertidal dolomitic limestones

L-2
Offshore siltstones, shales and limestones

L-1
Nearshore sandstones minor dolomitized limestones

Well 7128/6-1

MD (m)

Gamma Ray
40 80 120 160

1640
1700
1800
1900
2000
2100

Seismic Units-Horizons

BTH
SU6
BKH
SU5
MSH
SU4
UAH
SU3
BAH
SU2
MGH
UCH
SU1
MCH

Colpaert et al. (2007)

Depositional sequences
Ehrenb. et al. (1998a)

3rd order | 2nd order

S-7
S-6
S-5
S-4
S-3
S-2
S-1

Gp (Fm)

Tempelfjorden Gp (Røye Fm)

Bjarmeland Gp
Isbjørn Fm

Gipsdalen Gp (Ørn Fm)

Gipsdalen Gp (Falk Fm)

Bio. ages
Ehrenb. et al. (2000)

Late Permian
—? Kungurian
late Artinskian
early Artinskian
l. Sakmarian
early Sakmarian
late Asselian
middle Asselian
e. Asselian
late Gzhelian
early Gzhelian

Lithotypes
- Anydrite
- Calcareous Sandstone
- Calcareous Claystone
- Calcareous Siltstone
- Silty Limestone
- Dolostone
- Limestone
- No Core

Lithofacies Associations (LA)
- LA1-Nodular Anhydrite
- LA2-Dolomitic Mudstones
- LA3-Fine-grained calcareous Sandstone
- LA4-Bioclastic Wackestone-Packstones
- LA5-Bioclastic Grainstones
- a b LA6-Skeletal Boundstones
- LA7-Fusulinid Wackestone-Packstones
- LA8-Crinoidal-Bryozoan Packstone-Grainstones
- LA9-Crinoidal-Bryozoan silty Wacke-Packstones

Major skeletals/non-skeletals
- Small Foramifera
- Green Algae
- Palaeoaplysina
- Colonial Corals
- Isolated Corals
- Phylloid algae
- Red algae
- Fusulinids
- Tubiphytes
- Bryozoans
- Crinoids
- Brachiopods
- Mollusks
- Gastropods
- Sp. spiculae
- Sponges
- Trilobites
- Peloids

Sedimentary Structures
- Pseudo-bedding
- Subaerial exposure
- Erosive surface
- Bioturbation

Depositional Cycles
- SB
- Shallow-Up
- MFS
- Deep-Up
- SB

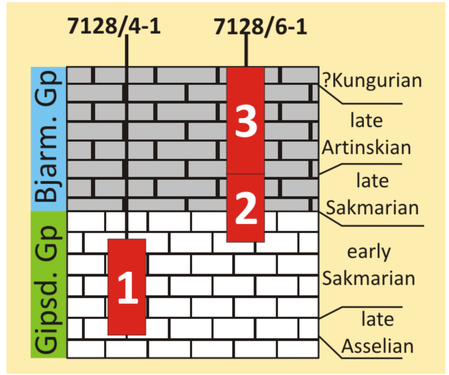

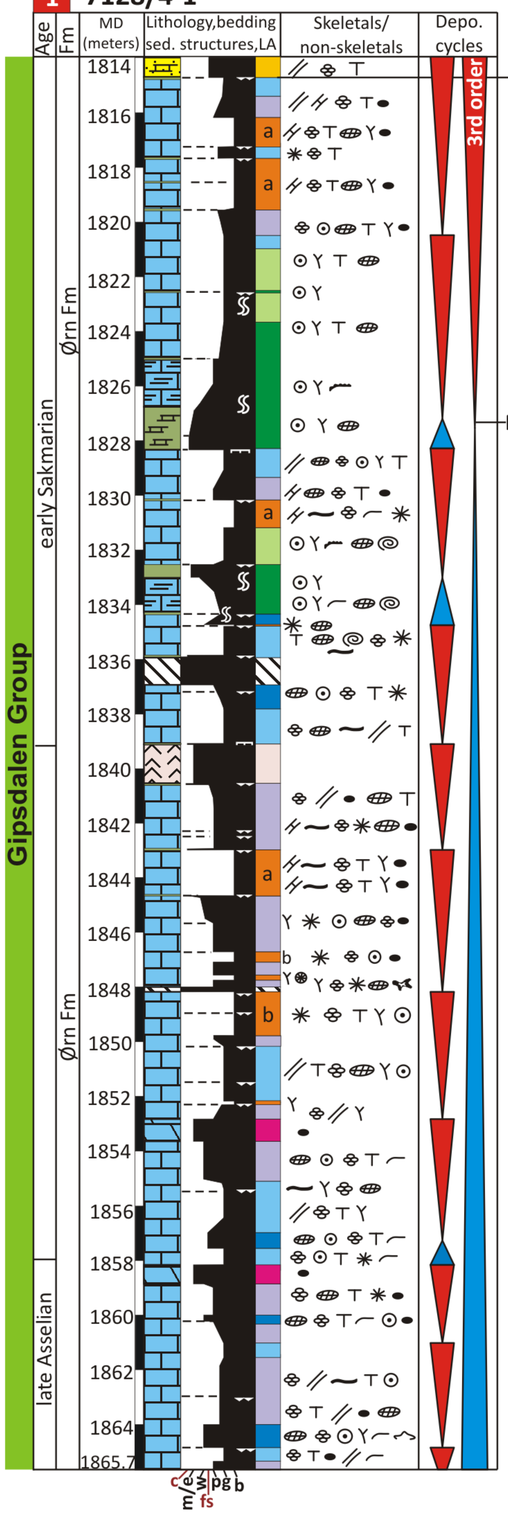

26.1 km

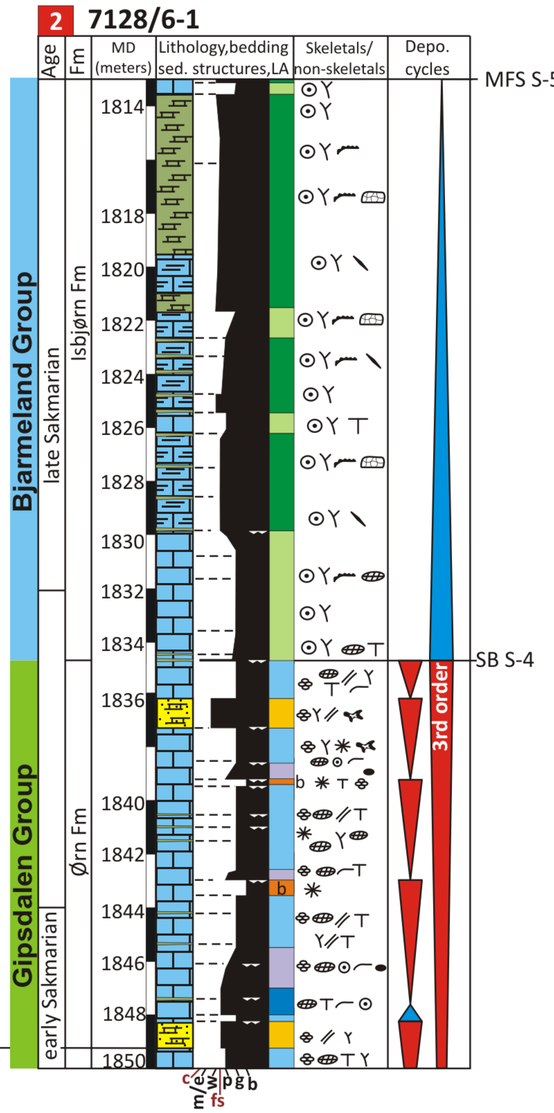

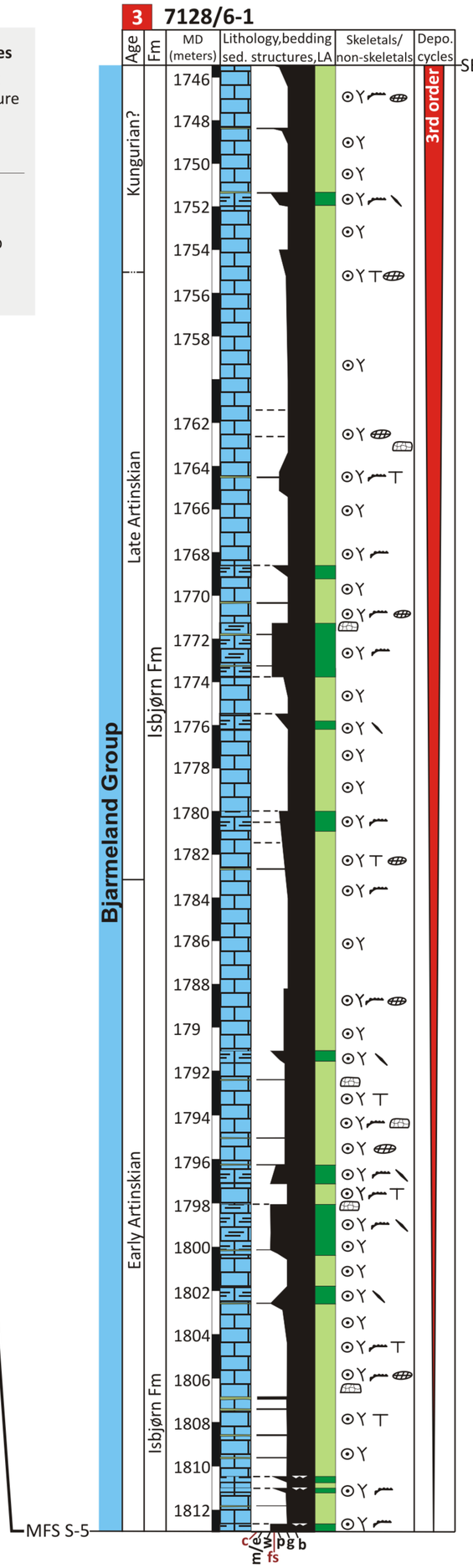

a

b

p
m
p
m
p

c

d

e

Isbjørn Fm

Ørn Fm

f

a

0,5 mm

b

1 mm

c

E

B

E

F

E

1 mm

d

T

T

G

E

T

F

1 mm

e

Gv

Gv

Gv

Gv

1 mm

f

K

1 mm

g

m

c

c

a

1 mm

h

G

Tx

G

t

1 mm

a

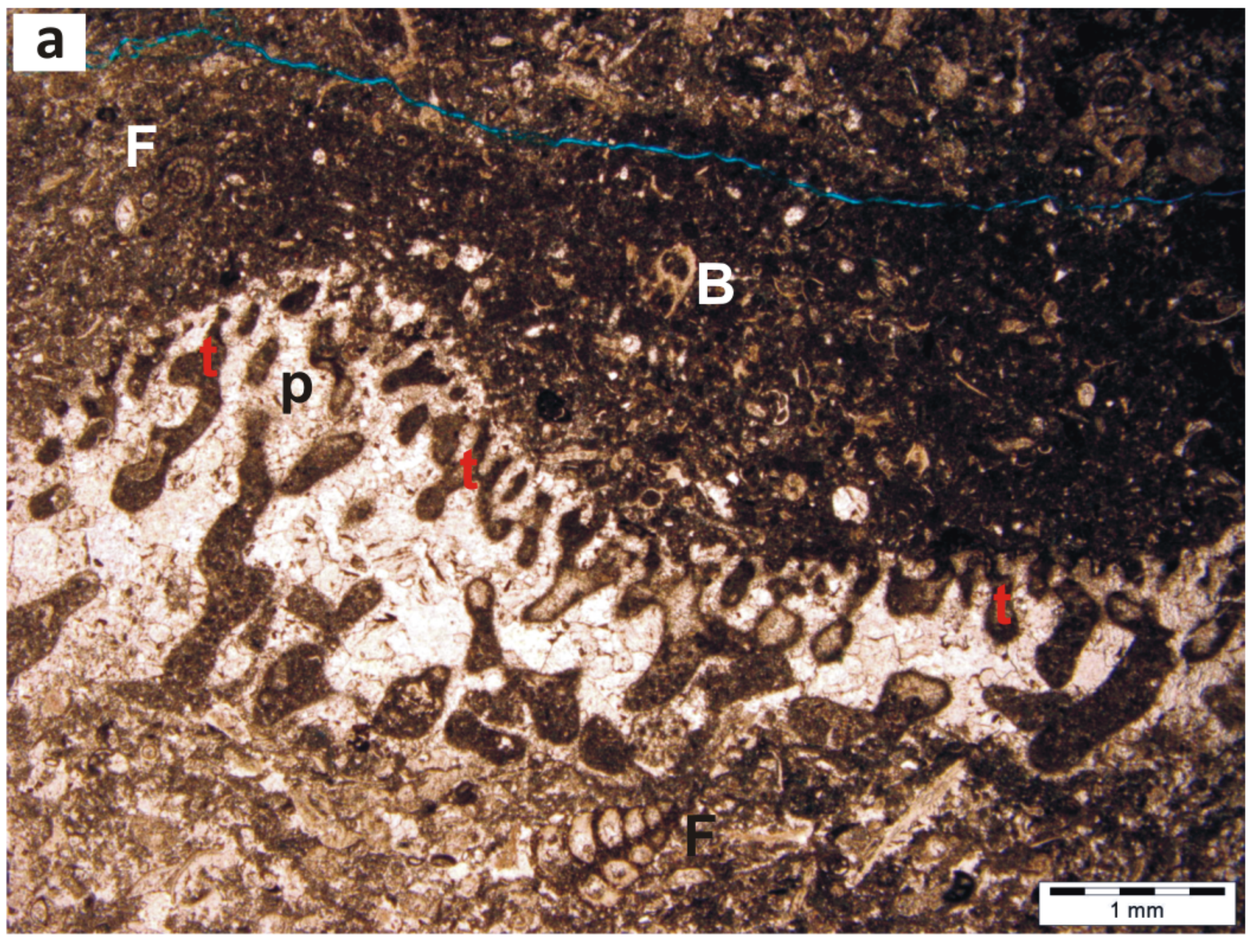
F
B
t
p
t
t
F
1 mm

b

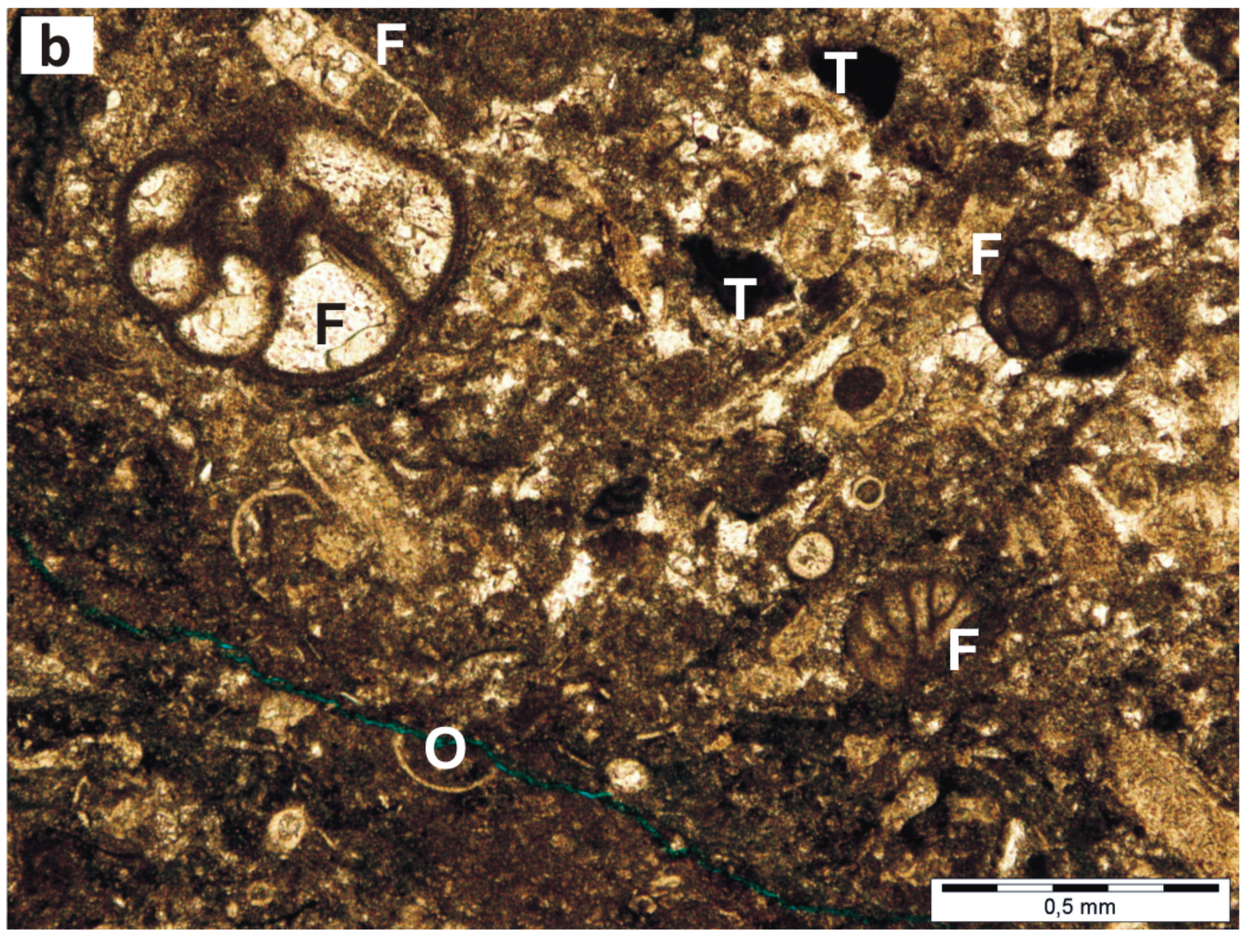
F
T
F
T
F
F
O
0,5 mm

c

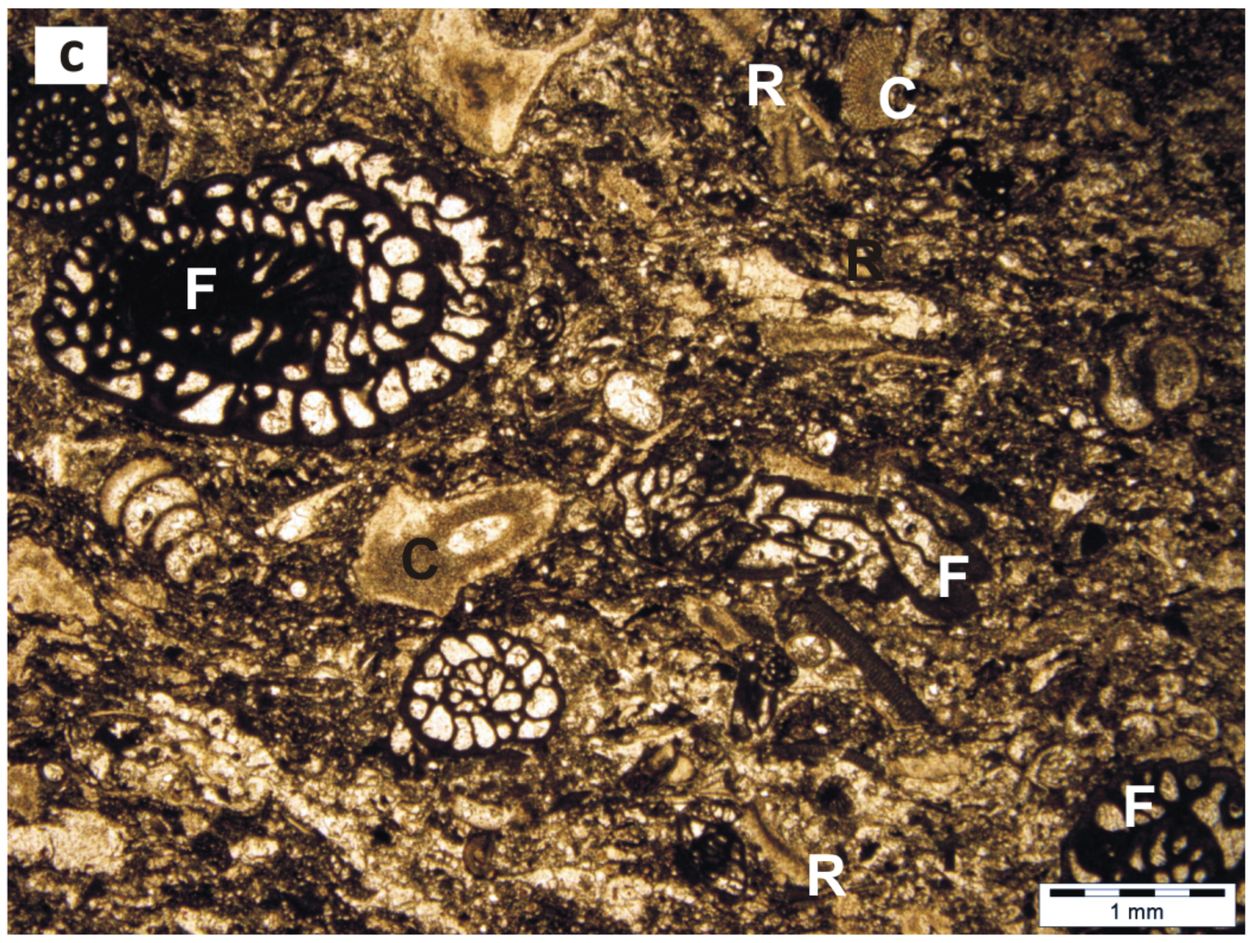
R
C
F
R
C
F
F
R
1 mm

d

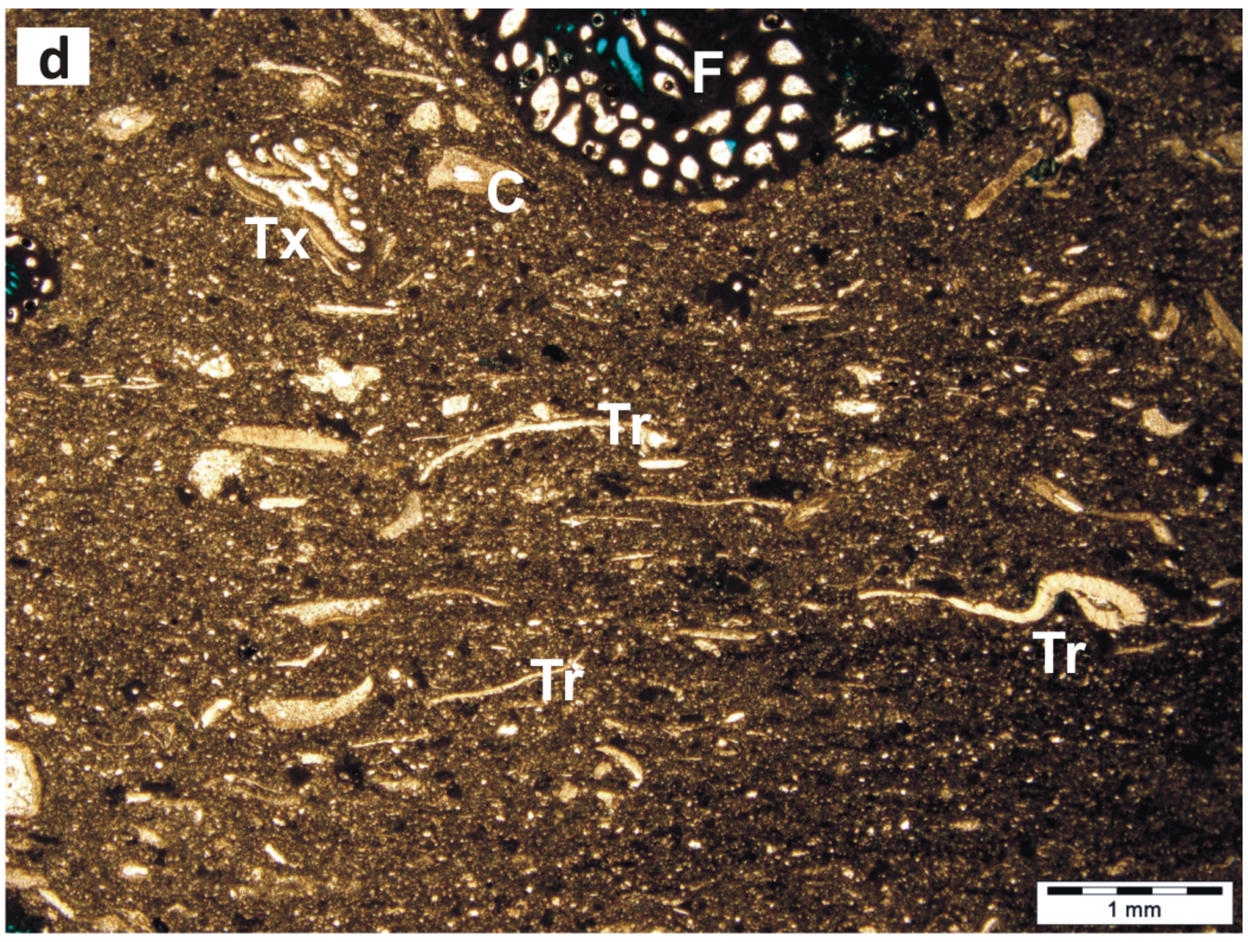
F
C
Tx
Tr
Tr
Tr
1 mm

e

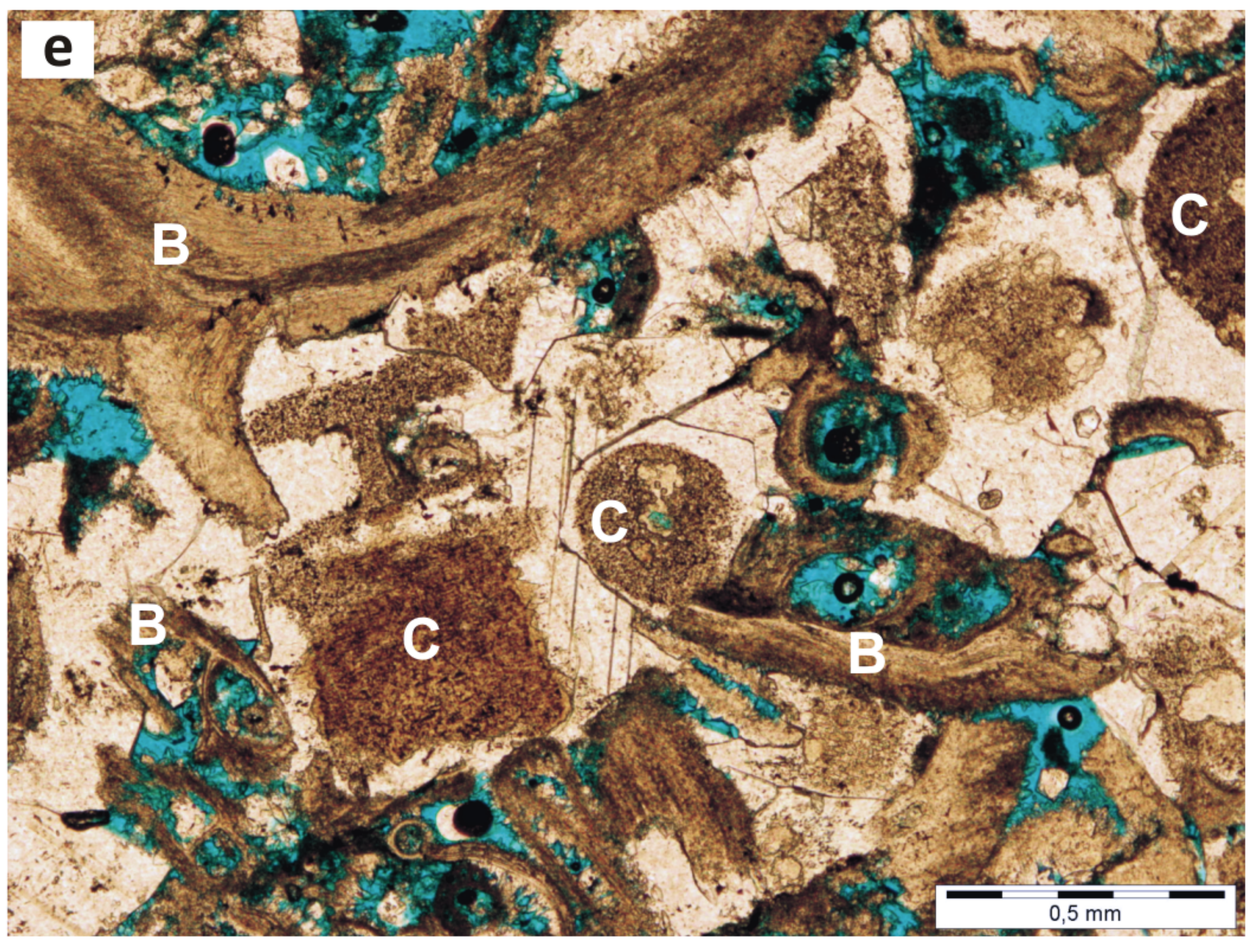
B
C
C
B
C
B
0,5 mm

f

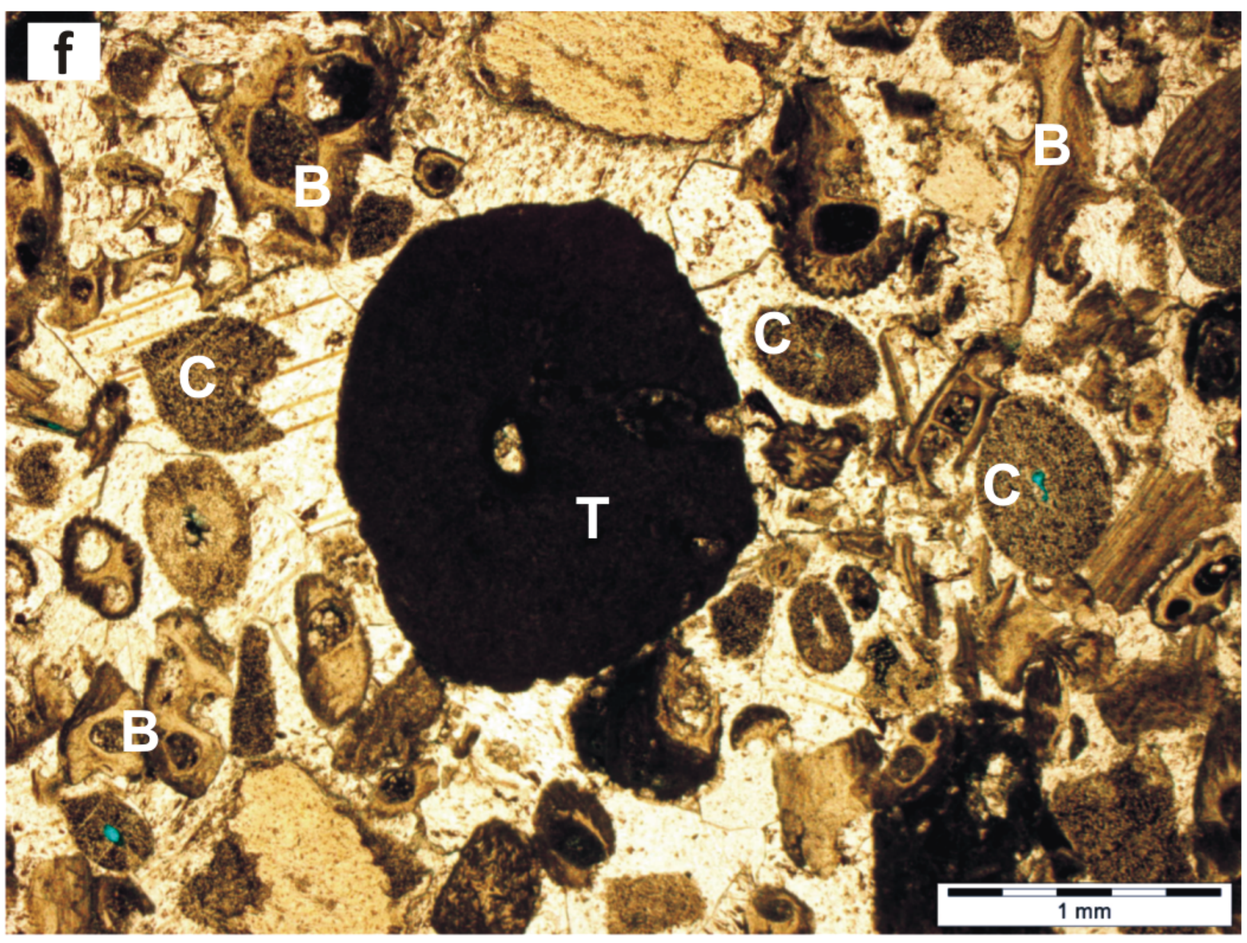
B
B
C
C
T
C
C
B
1 mm

g

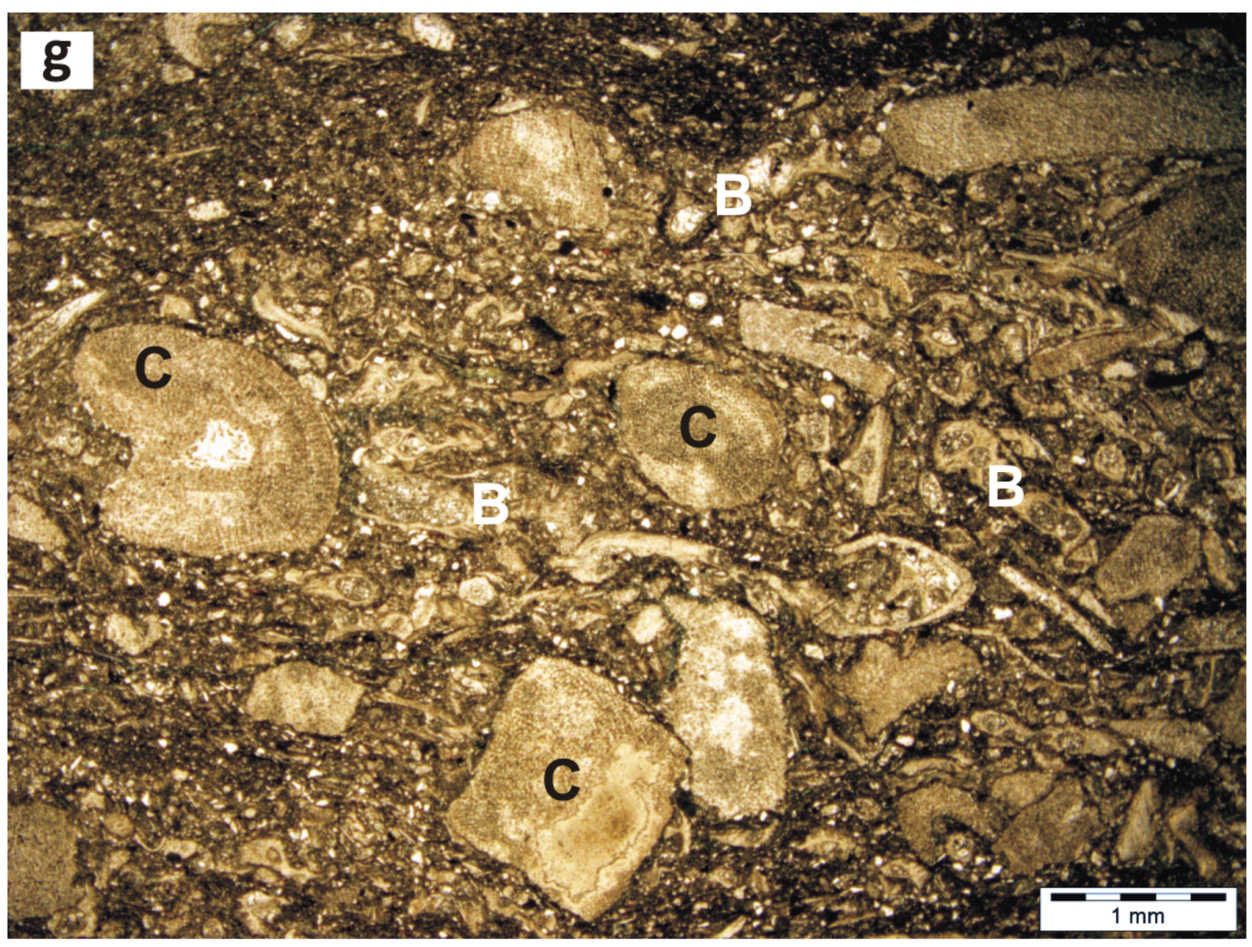
B
C
C
B
B
C
1 mm

h

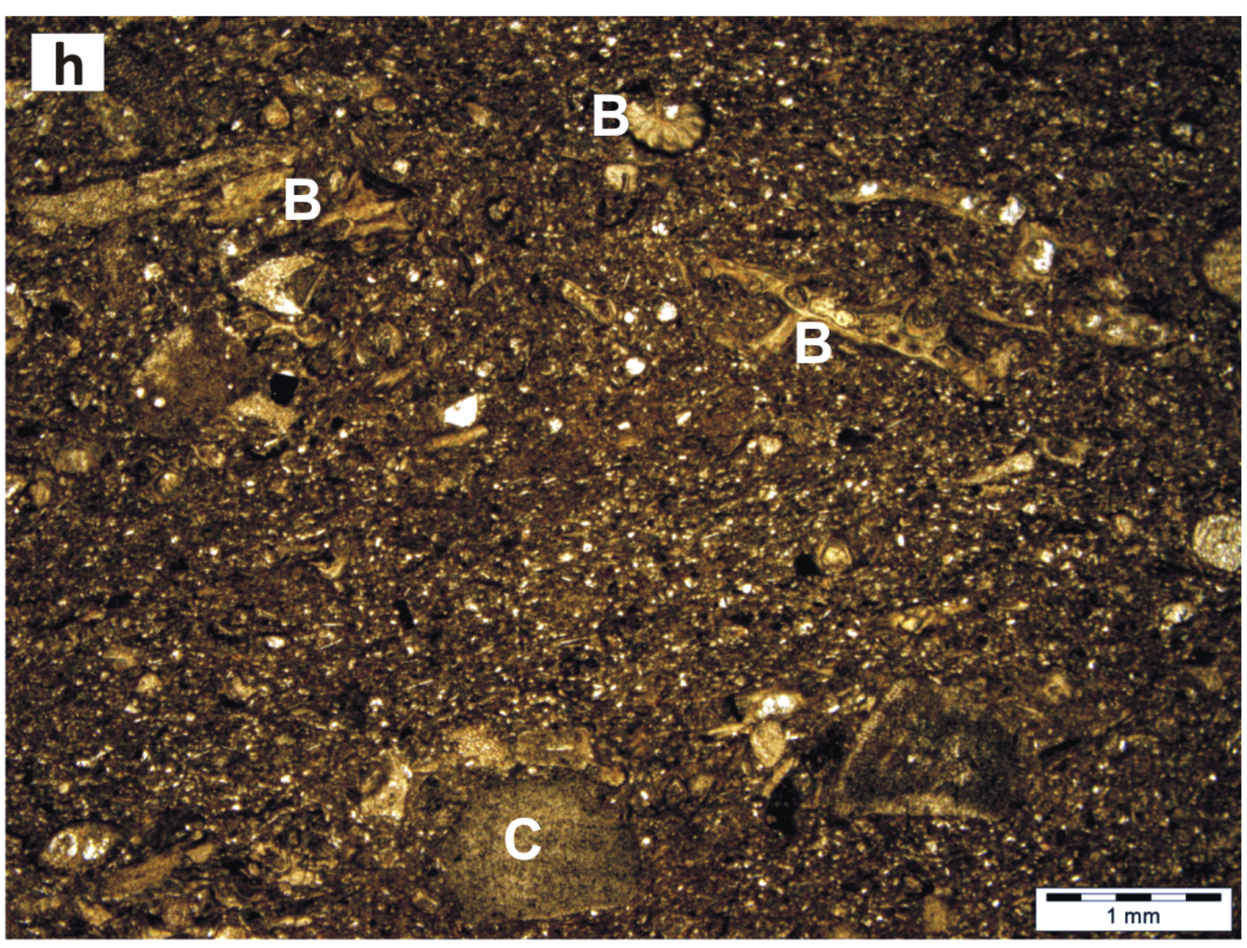
B
B
B
C
1 mm

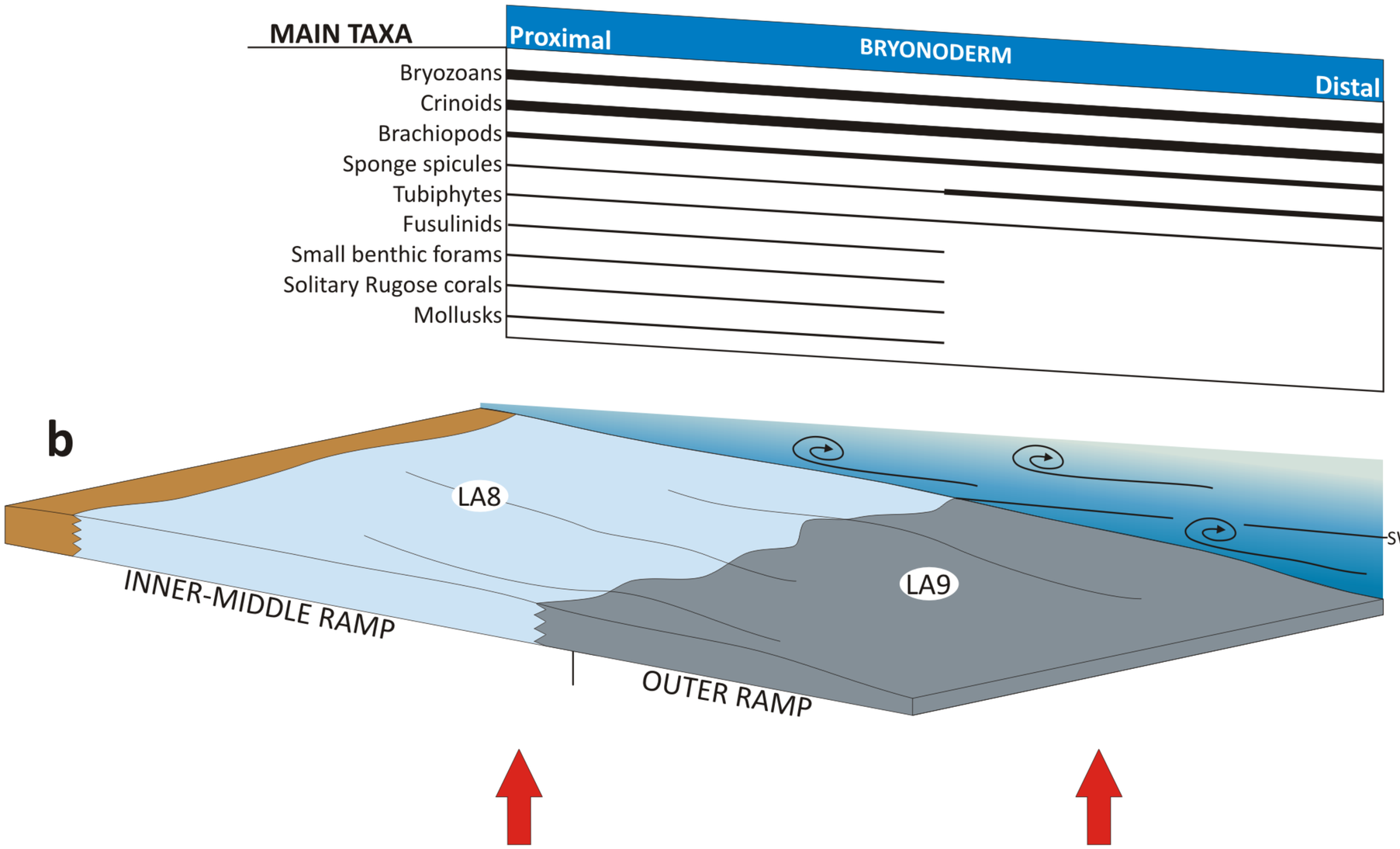

late Sakmarian - late Artinskian
Isbjørn Fm (Bjarmeland Group)

-Temperate latitudinal belt.
-Low ampl./frequency sea-level fluctuations.
-Poor stratified sea-water column and open circulation across the platform.
-Enhanced upwelling of cooler waters and trophism.
-Bryonoderm sedimentation mode.

Legend

- Continentally-influenced inner ramp
- Storm-dominated inner-middle ramp
- Offshore domain

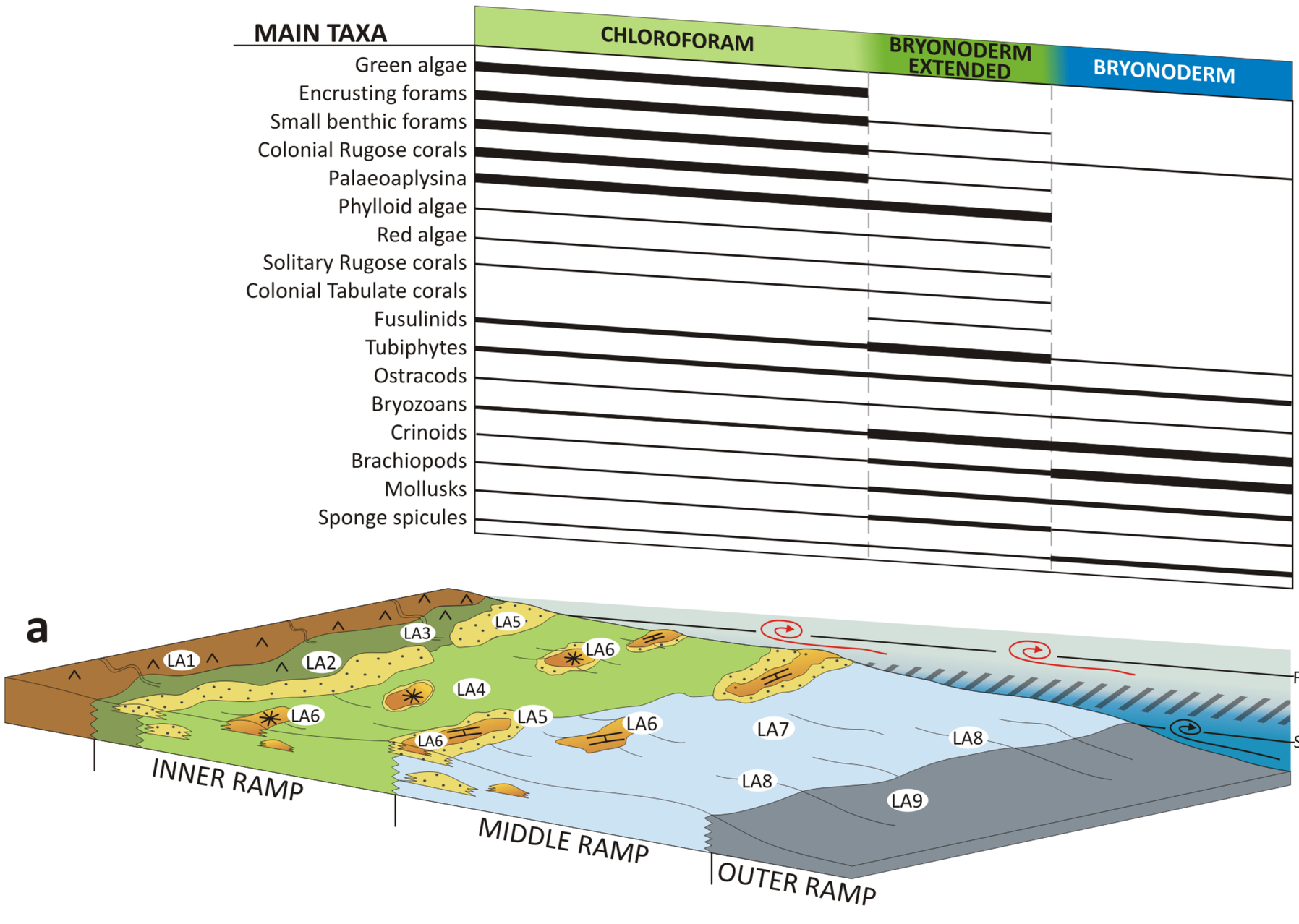

Late Gzhelian-Early Sakmarian
Ørn Fm (Gipsdalen Group)

-(Sub)tropical latitudinal belt.
-Glacio-eustatic influence with cyclic meteoric exposure of proximal domains.
-Stratified water column (stable termocline) with warm surperficial waters and cooler mid to outer shelf domains.
-Depth-related shift from Chloroforam to Bryonoderm sedimentation mode.

Legend

- Supratidal sabhka
- Restricted tidal flat/shallow lagoon
- Skeletal banks/shoals
- Partially protected shallow lagoon
- Open subtidal
- Offshore
- Coral boundstones
- Palaeoaplysina boundstones
- Warm oligotrophic water circulation
- Cool mesotrophic water circulation
- Thermocline interval

Relative skeletal abundance

- Frequent
- Common
- Rare

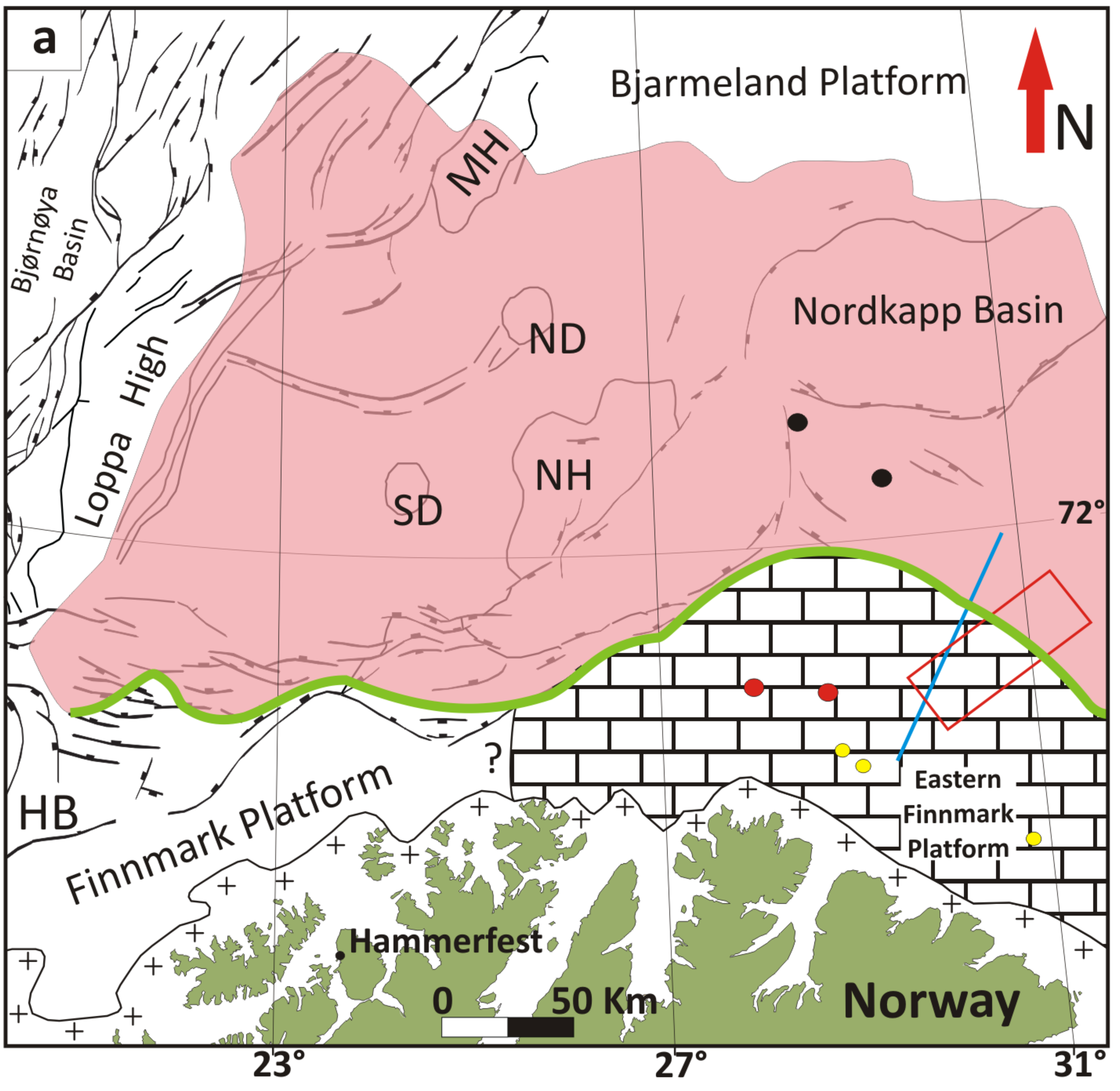

Gzhelian-Asselian platform domain

Gzhelian-Asselian lowstand basinal evaporites

Palaeo-margin

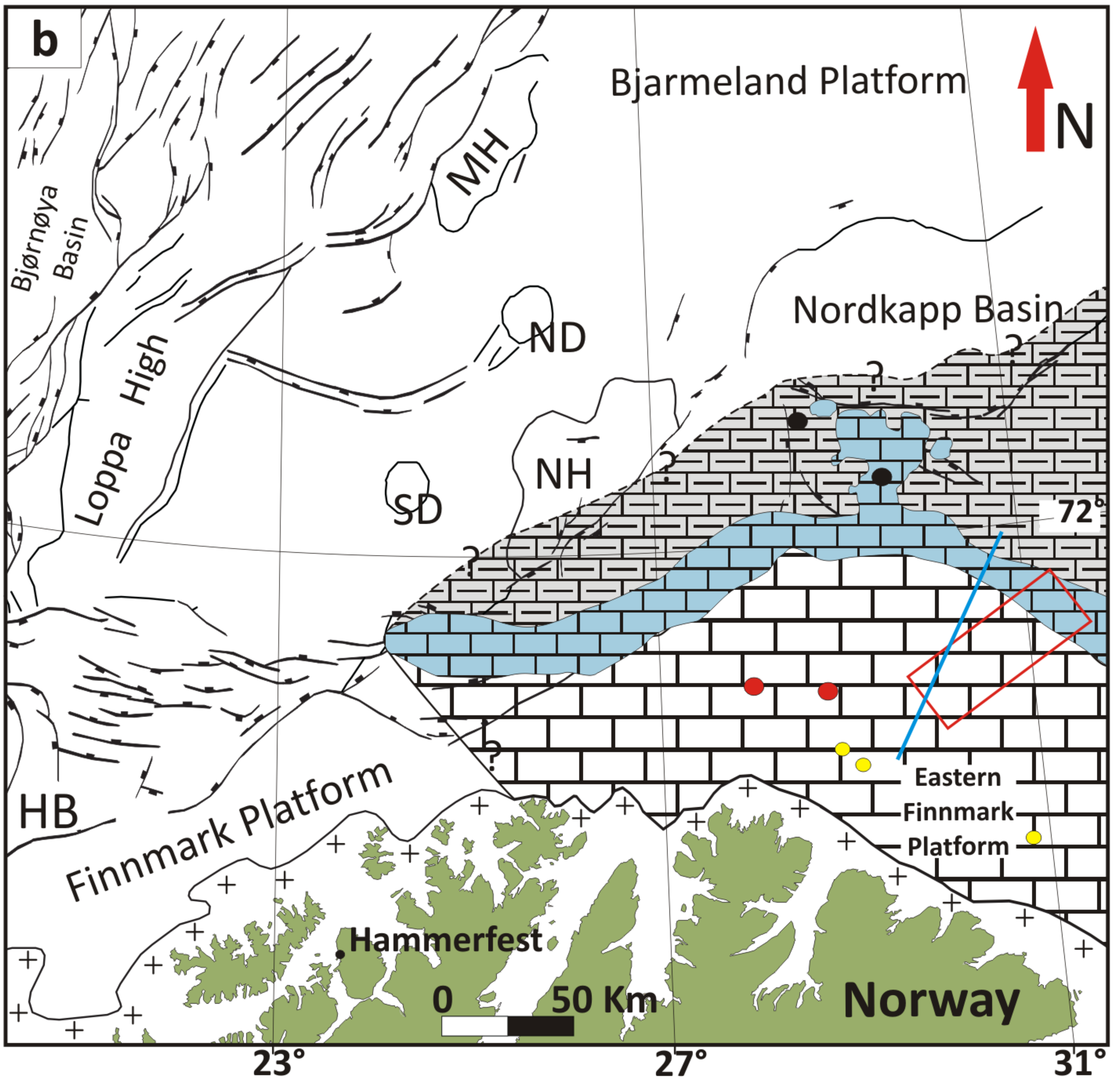

Sakmarian-Artinskian platform domain (Isbjørn Fm)

Stacked buildup complexes (Polarrev Fm)

deep silty mudstones (Ulv Fm)

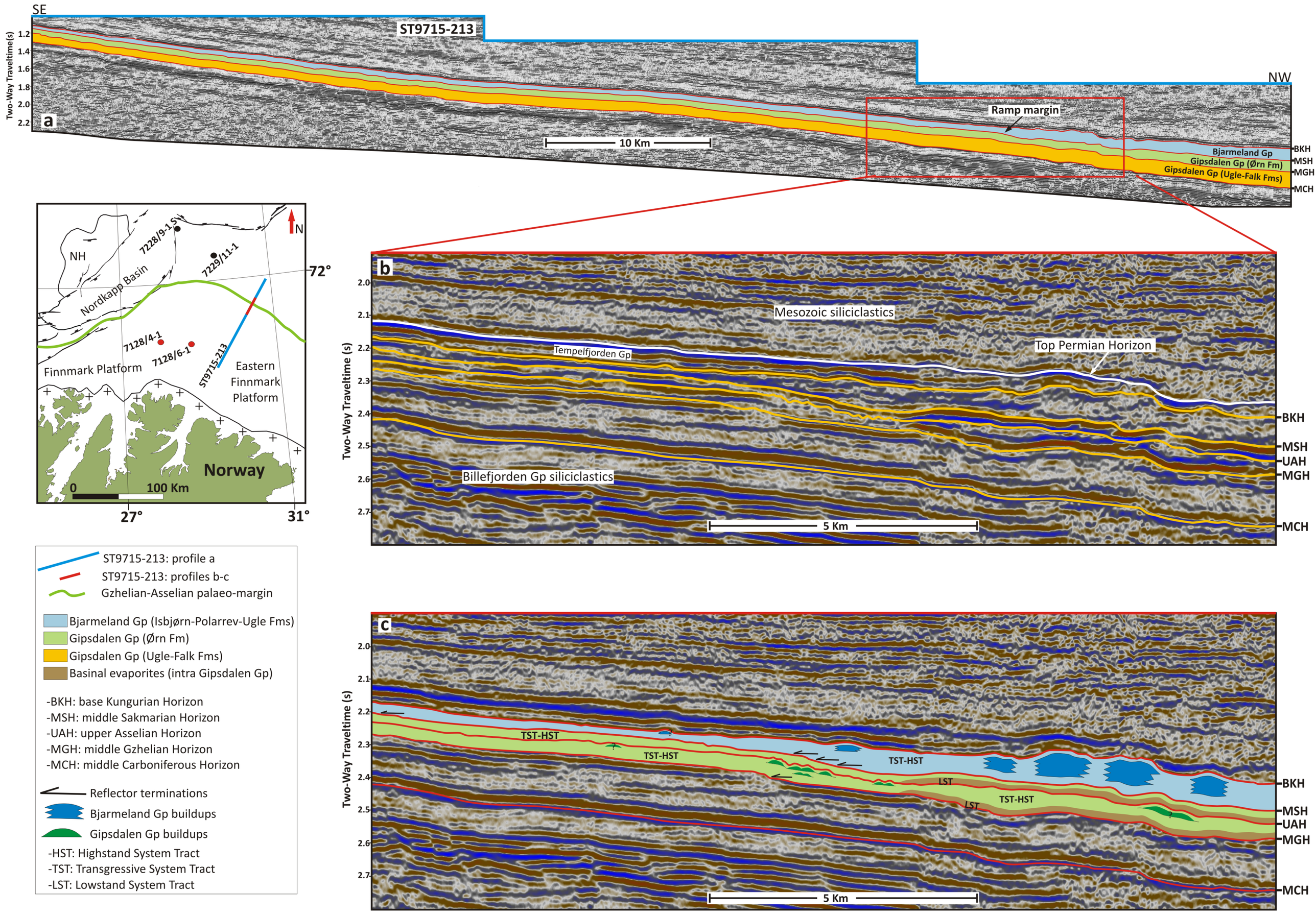
SE
NW
ST9715-213
Two-Way Traveltime (s)
1.2
1.4
1.6
1.8
2.0
2.2
a
10 Km
Ramp margin
Bjarmeland Gp
Gipsdalen Gp (Ørn Fm)
Gipsdalen Gp (Ugle-Falk Fms)
BKH
MSH
MGH
MCH
N
NH
7228/9-1 S
7229/11-1
Nordkapp Basin
72°
7128/4-1
7128/6-1
ST9715-213
Finnmark Platform
Eastern
Finnmark
Platform
Norway
0
100 Km
27°
31°
b
Mesozoic siliciclastics
Tempelfjorden Gp
Top Permian Horizon
Billefjorden Gp siliciclastics
5 Km
C
TST-HST
TST-HST
TST-HST
LST
LST
TST-HST
?
?
5 Km
ST9715-213: profile a
ST9715-213: profiles b-c
Gzhelian-Asselian palaeo-margin
Bjarmeland Gp (Isbjørn-Polarrev-Ugle Fms)
Gipsdalen Gp (Ørn Fm)
Gipsdalen Gp (Ugle-Falk Fms)
Basinal evaporites (intra Gipsdalen Gp)
-BKH: base Kungurian Horizon
-MSH: middle Sakmarian Horizon
-UAH: upper Asselian Horizon
-MGH: middle Gzhelian Horizon
-MCH: middle Carboniferous Horizon
Reflector terminations
Bjarmeland Gp buildups
Gipsdalen Gp buildups
-HST: Highstand System Tract
-TST: Transgressive System Tract
-LST: Lowstand System Tract